ABSTRACT

RAGHU, AMRUTHA. Reaction Paths for Hemicellulose Pyrolysis Using Reactive Molecular Dynamics. (Under the direction of Dr. Phillip R. Westmoreland)

This study is focused on understanding the pyrolysis of beechwood xylan, a type of hemicellulose, using Reactive Molecular Dynamics simulations to predict the reaction pathways involved in the pyrolysis process, to study the yields as functions of temperature, and to evaluate the accuracy of LAMMPS/ReaxFF predictions. Calculations were performed on an isothermal-isobaric system of β-D-xylopyranose to emulate a Py-GCxGC/ToFMS experiment elsewhere in the Westmoreland lab. The pyrolyses of beechwood xylan and its monomer β-D-xylopyranose were meant to provide identities and yields of the products formed, which were then the bases of model comparisons. The most frequent reactions predicted by the simulations were analyzed using quantum-chemical density functional theory to deduce the probability of occurrence of the reaction pathway. The products generated from simulations were compared to the product distributions obtained from experiments to understand the underlying chemistry and factors driving the process.

Products observed in the Py-GCxGC/ToF MS experiment that have been detected in ReaxFF MD calculations are glyceraldehyde, D-xylose, and glyoxal. Ethene-1,2-diol, (E)-3-hydroxyacrylaldehyde, and (2R,3S,4R)-3,4-dihydroxytetrahydrofuran-2-carbaldehyde are also detected in NPT ReaxFF MD calculations that are structurally similar to glycolaldehyde, 1-hydroxypropan-2-one, and furfural respectively, which are major products that have useful chemical applications.

Reaction Paths for Hemicellulose Pyrolysis Using Reactive Molecular Dynamics

by

Amrutha Raghu

A thesis submitted to the Graduate Faculty of
North Carolina State University
in partial fulfillment of the
requirements for the degree of
Master of Science

Chemical Engineering

Raleigh, North Carolina

2018

APPROVED BY:

_____	_____
Phillip R. Westmoreland Committee Chair	Erik E. Santiso
_____	
Donald W. Brenner	

BIOGRAPHY

Amrutha Raghu was born in Tamil Nadu, India. She received her B. Tech degree in chemical engineering at National Institute of Technology, Tiruchirapalli in India from 2013 to 2017. During the course of the undergraduate study she had done summer internship at TATA Chemicals, Gujarat as a sophomore and a research internship at Indian Institute of Science Bangalore under the guidance of Dr. Ganapathy Ayappa in department of chemical engineering in junior year. She had learnt fundamentals behind process design salt manufacturing at the TATA Chemicals plant. She had worked on simulation of adsorption of methane gas on graphine oxide using Grand Canonical Monte Carlo simulation in Dr.Ganapathy Ayappa's lab in chemical engineering department to optimize the process and develop profound understanding in membrane design. In 2017, she joined as a graduate student at North Carolina State University and became a research assistant at the Westmoreland lab. She has been investigating the hemicellulose pyrolysis reaction chemistry using Reactive Molecular Dynamics under the guidance of Dr. Phillip Westmoreland.

ACKNOWLEDGEMENTS

I would like to express my profound gratitude to my advisor Dr. Phillip R. Westmoreland for the guidance and constant encouragement to pursue my thesis research goal. His vision for research in biomass pyrolysis and my role in it fueled my passion for making a significant contribution in this field and has been a constant source of motivation.

I am grateful to Mr. Arnab Bose and Mr. Charles McGill for their invaluable insights and for constantly checking up on me and steering me in the right direction. The whole Westmoreland group has played an integral role in making this research successful.I also appreciate the helpful comments of my committee members, Professors Brenner and Santiso.

I would also like to thank Mr. Chowdhury Mahbub Ashraf and Dr. Adri van Duin from Penn State University for their inputs and technical expertise in molecular dynamic simulation.

This research would not have been possible without the support and infrastructure provided by the Office of Information Technology at North Carolina State University. I extend sincerest thanks to my parents, friends and family for their never-ending support.

TABLE OF CONTENTS

LIST OF FIGURES

CHAPTER 1: INTRODUCTION

Exploitation of conventional fuels for several decades and increase in demand for energy has created a pressing need for sustainable, affordable, and environmentally friendly sources of renewable energy. Biomass constitutes the organic waste generated by industries, and agriculture can be a viable source of renewable energy. Fast pyrolysis of biomass is a process in which the biomass is heated in absence of oxygen at an elevated temperature (typically around 500^{o}C) with a very high heating rate to produce bio-oil and other useful chemical products [1]. Bio-oil has high potential to be a source of alternative fuel; therefore, biomass pyrolysis has received tremendous attention in the last decade.

Lignocellulosic plant biomass can be classified as lignins, cellulose, and hemicellulose. Significant progress has been made in experimental techniques for understanding the pyrolysis process using drop-tube furnaces, Dauenhauer's PHASR reactor, and micropyrolyzer reactors [1], combined with chromatographic and mass-spectrometric methods. The characterization of results from these experiments has led to development of empirical kinetic models for pyrolysis of each of the three major components of biomass. These models describe the overall kinetics of the system but are not sufficient to describe the detailed chemistry and selectivity taking place during the pyrolysis reactions.

Understanding the reaction chemistry is crucial in developing reactors to optimize the production of desired products. Therefore, in addition to experimental results, computational methods such as quantum chemistry calculations and Reactive Molecular Dynamics will be relied upon to shed more light into the reaction pathways governing pyrolysis of biomass reactions.

1.1 Research outline

The goal of the thesis work is to develop an efficient approach to predict reaction pathways involved in pyrolysis of hemicellulose using Reactive Molecular Dynamics with ReaxFF force field. Ideally, it would justify the product distribution observed from Py-GCxGC/ToFMS experiments conducted in the Westmoreland lab. The biomass taken for the study is beechwood xylan. Hemicellulose can be broadly classified as glucans, mannans, galactans, and xylans. It is present in the plant cell wall and is an amorphous polymer [1]. Due to the amorphous nature and high variability in structure from source to source, hemicellulose pyrolysis involves complex chemistry leading to chemically useful products. As the molecular structure of beechwood xylan is unknown, it is speculated that β-D-xylopyranose could be the monomer [2] and hence it could lead formation of the major products observed in the pyrolysis. The pyrolysis of β-D-xylopyranose is carried out along with xylan which is then compared to product distribution obtained from the Reactive Molecular Dynamics calculations.

The pyrolysis reactions are carried out in a Pyroprobe-GCxGC/ToFMS apparatus by heating a known amount of sample at the rate of 1000ºC/min in absence of oxygen. The gaseous products from the pyrolysis reaction are separated using two-dimensional gas chromatography. As they elute, molecules are first ionized in the mass spectrometer by collision of high-energy electrons, generating a mass spectrum of fragments at each moment of elution. For a given electron energy, the mass spectrum of a molecule is typically unique, which is helpful in identifying the products.

Reactive Molecular Dynamics is used to simulate the pyrolysis process for a given isothermal-isobaric pyrolysis system of molecules. In principle, it will predict the reaction pathways and determine the transition structures from reactant(s) to product(s) that occur during

the course of a reaction. The probability of a given reaction pathway happening at the given conditions is determined from molecule kinetic and rotational energies, molecular configurations, and the forces between atoms within and between molecules. These force fields are either fitted to data or derived from quantum chemistry calculations.

After the simulation, further quantum chemistry calculations are carried out to seek the transition structure that is implied by Reactive Molecular Dynamics calculations for a given reaction. If such a transition state is identified, a quantum-mechanical Intrinsic Reaction Coordinate calculation is conducted to establish the corresponding reaction reactant(s) and product(s) based on the minimum-energy path taken to form the reactant(s) and product(s) from the optimized transition state. The minimum-energy pathway calculated also shows the minimum energy required to form the transition state. This result establishes whether an inferred reaction pathway corresponds to a quantum-chemical transition state.

CHAPTER 2: MOLECULAR DYNAMICS

2.1 Introduction

Molecular dynamics is a computational technique that can simulate the behavior of atoms and molecules in real time and space by determining the interatomic forces with evolution of time using Newton's second law of motion. This technique can be used to understand the phenomena behind physical systems such as polymer degradation, molecular docking for drug development, annealing of crystals to membrane design for gas adsorption, and for observing chemical reactions in processes such as combustion and pyrolysis.

The interatomic forces between the atoms are determined from the potential energy of the system that is specifically designed to capture a phenomenon. Newton's second law of motion is numerically evaluated using time-integration techniques such as the Verlet algorithm [3] for each atom in the system in all three directions, determine the position and velocity throughout the course of simulation. The study of dynamics of all atoms in the system can reveal comprehensive information about the system, regardless of type of phenomena. The experimental conditions are replicated in the simulation by developing a relationship between the microscopic properties such as position and velocity of an atom and measurable macroscopic properties such as pressure, volume, and temperature, given by statistical mechanics [4].

The potential energy model consists of bonded interactions and non-bonded interactions. Bonded interactions could arise due to potential energy stored in molecules in its bonds, angles, and dihedrals, whereas non-bonded interactions occur due to dipole-dipole interactions, columbic interactions, hydrogen bonding, etc. The weightage of each interaction in the dynamics of the molecule depends on many factors such as its structural properties, ensemble properties specified by statistical mechanics, and its interaction with neighboring molecules.

A brief outline for execution of molecular dynamics is shown below:

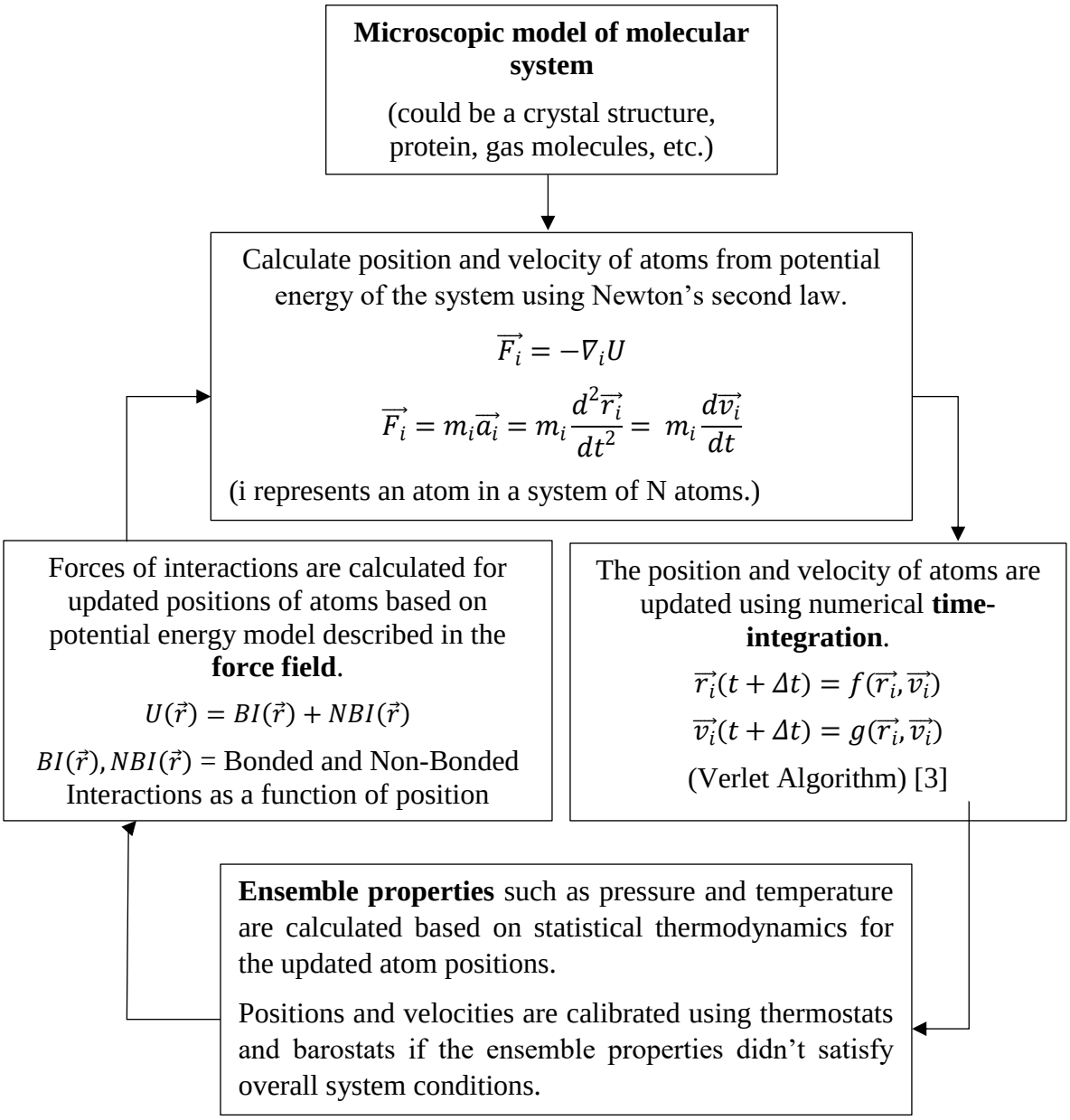

Figure 2.1 General algorithm for execution of molecular dynamics.

2.2 Time-integration technique

Evaluation of Newton's second law of motion is not computationally feasible for all atoms in a system (a system of differential equations with initial value constraints) for every small interval of

time. In order to reduce the computational expense, numerical techniques are employed to integrate Newton's second law with respect to time. The choice of integrator affects the simulation outcome significantly as the potential energy is very sensitive to position of atoms. A small perturbation in energy could lead to dramatic change in the atom positions. As numerical integration involves discrete approximation of differential equations (Newton's second law), so the integrator of choice should enable the system to be stable for small fluctuations of atom positions [5]. The time-integration technique should also ensure conservation of energy and momentum at every timestep throughout simulation [6]. Numerical integration techniques commonly used for implementation of molecular dynamics include the leap-frog method, Verlet, Velocity-Verlet algorithm, and Beeman algorithm. The integrator chosen in the study is the Velocity-Verlet algorithm.

2.2.1 Verlet and Velocity-Verlet algorithm

Discrete approximation of Newton's second law of motion for all atoms is based on a Taylor series expansion. This approach was developed by Verlet [3] to calculate physical and thermodynamic properties of argon that vary with time; namely pressure, temperature, internal energy, elastic moduli, and isotopic separation factor as a function of Ar position. For a discrete time interval Δt, the updated positions and velocities can be expressed as shown below:

$$r_i(t+\Delta t) = r_i(t) + \Delta t\frac{dr_i}{dt} + \frac{\Delta t^2}{2!}\frac{d^2r_i}{dt^2} + \frac{\Delta t^3}{3!}\frac{d^3r_i}{dt^3} + 0(n^4) \qquad \textbf{2-iv}$$

$$r_i(t-\Delta t) = r_i(t) - \Delta t\frac{dr_i}{dt} + \frac{\Delta t^2}{2!}\frac{d^2r_i}{dt^2} - \frac{\Delta t^3}{3!}\frac{d^3r_i}{dt^3} + 0(n^4) \qquad \textbf{2-ii}$$

The limit derivative of position (velocity) with respect to time is defined as:

$$v_i(t) = \lim_{\Delta t\to 0}\frac{r_i(t+\Delta t) - r_i(t)}{\Delta t} \qquad \textbf{2-viii}$$

which can also be written as:

$$v_i(t) = \lim_{\Delta t \to 0} \frac{r_i(t) - r_i(t - \Delta t)}{\Delta t} \qquad \textbf{2-iv}$$

Therefore, by using equations 2-i, 2-ii, 2-iii and 2-iv, one can arrive at an expression for velocity that can be numerically evaluated by Equation 2-v:

$$v_i(t) = \lim_{\Delta t \to 0} \frac{r_i(t + \Delta t) - r_i(t - \Delta t)}{2\Delta t} \qquad \textbf{2-v}$$

Adding equations 2-i and 2-ii gives

$$r_i(t + \Delta t) + r_i(t - \Delta t) = 2r_i(t) + \frac{\Delta t^2}{2!} a_i(t) \qquad \textbf{2-vi}$$

$$a_i(t) = \frac{F_i(t)}{m_i} \qquad \textbf{2-vii}$$

Equation 2-vi can be rewritten as:

$$r_i(t + \Delta t) + r_i(t - \Delta t) = 2r_i(t) + \frac{\Delta t^2}{2!} \frac{F_i(t)}{m_i} \qquad \textbf{2-viii}$$

In order to make time discrete for computationally evaluating equation 2-viii, Δt can be expressed as the time interval between consecutive times at which dynamics of the system is evaluated, the timestep:

$$\Delta t = t_{n+1} - t_n$$

Equation 2-viii can be rewritten as:

$$r_i(t_{n+1}) = 2r_i(t_n) - r_i(t_{n-1}) + \frac{\Delta t^2}{2!} \frac{F_i(t_n)}{m_i} \qquad \textbf{2-ix}$$

Discretizing time as shown in equation 2-ix is known as the Verlet algorithm**,** which relies on data obtained in two previous steps t_n and t_{n-1} to determine the dynamics of system at the next step [3].

The Velocity-Verlet algorithm was developed in 1982 to reduce computational cost further, as this algorithm needed data of only the previous dynamics of the system and it evaluated velocity simultaneously with position [7] [8].

The position is evaluated using time discretization of equation 2-i:

$$r_i(t_{n+1}) = r_i(t_n) + \Delta t v_i(t_n) + \frac{\Delta t^2}{2!}\frac{F_i(t_n)}{m_i} \qquad \textbf{2-x}$$

$$v_i(t_{n+1}) = v_i(t_n) + \left(\frac{a_i(t_n) + a_i(t_{n+1})}{2}\right)\Delta t \qquad \textbf{2-xi}$$

With knowledge of $r_i(t_{n+1})$, force $F_i(t_{n+1})$ at t_{n+1} can be evaluated from the interaction potential, from which $a_i(t_{n+1})$ can be deduced. Equation 2-xi was derived analytically using position and velocity at an intermediate timestep $(\Delta t/2)$, and the unknown terms were eliminated using the limit definition of acceleration like Verlet algorithm. The advantage of this algorithm over the Verlet algorithm is that memory use is less, thereby increasing the computational speed.

2.2.2 Choice of timestep

The choice of timestep directly affects intricacy of knowledge about the dynamics of system and the computational speed of calculations. In order to achieve a smaller computational time, it is natural to choose a larger timestep, but there is a limitation to choose a larger timestep. Molecular dynamics can fail when a system of particles becomes unstable due to large truncation error in the integration process, such that total energy of the system may rapidly increase with time. As a result, molecules would not have a proper structure. This phenomenon is known as explosion and is caused by "devastating atomic collisions that occur when a large time step propagates the positions of two atoms to be nearly overlapping; the interaction creates a strong repulsive force repelling

these atoms far apart" [9]. Therefore, it is advisable to choose a smaller timestep to observe minute changes in dynamics based on the ensemble properties.

2.3 Role of statistical mechanics

Statistical mechanics provides a quantitative relationship between microscopic properties and macroscopic properties. In the quest to understand the variation in experimentally measurable properties due to phenomena observed in microscopic states, it was concluded that macroscopic observables are not significantly affected by the detailed dynamic motion of every particle in a macroscopic system; rather, it depends on collective average properties of the system, which eliminates microscopic details. The first breakthrough in theoretical understanding of statistical mechanics was realized using the concept of an ensemble.

2.3.1 Ensemble

An ensemble is defined as a collection of microscopic states that all realize an identical macroscopic state [8]. Consider a large number of replicas under a microscope, which interact with each other but are isolated from rest of the universe. Some of these replicas might have different configurations in terms of atom positions in the system but realize the same macroscopic properties such as energy of the ensemble. The number of microstates (replicas) that realize a macroscopic property is directly affected by the dynamics of atoms in these microstates. The probabilities of occurrence of all microstates are equal, but the probability of microstates having same energy is directly proportional to stability of the system at that energy [10]. This relationship is quantified by the partition function defined in statistical mechanics, which establishes a relationship between macroscopic properties measured and microscopic state of system. The concept of ensemble considers these microstates realizing the same macroscopic properties to be indistinguishable. A

fundamental assumption in statistical mechanics is that macroscopic properties conserved over time are affected only by change in dynamics of the system.

Using the laws of thermodynamics, the partition function is related to various macroscopic properties such as pressure and temperature. From the First and Second Laws of classical thermodynamics, it is known that

$$dE = T\,dS - P\,dV + \sum_{i=1}^{n} \mu_i\,dN_i \qquad \textbf{2-xii}$$

where *E, S, T, P, V,* μ are the internal energy, entropy, temperature, pressure, volume, and chemical potential of the system with N atoms. In a system with constant *N, V,* and *E*, entropy of the system is a function of *N, V,* and *E* only. Boltzmann and Planck devised a relation between entropy *S* and the number of microstates realizing a macroscopic state **Ω**:

$$S(N,V,E) = k \ln \Omega(N,V,E) \qquad \textbf{2-xiii}$$

where **Ω** is defined as the partition function and the constant *k* appearing in the equation 2-xiii is known as Boltzmann's constant, which is equal to 1.3806505(24) x $10^{-23} JK^{-1}$ [8]. From equation 2-xii, the following relations can be deduced:

$$\left(\frac{dS}{dE}\right)_{N,V} = \frac{1}{T}$$

$$\left(\frac{dS}{dV}\right)_{N,E} = \frac{P}{T}$$

$$\left(\frac{dS}{dN}\right)_{E,V} = \frac{\mu}{T}$$

Therefore macroscopic properties such as pressure, temperature, and chemical potential can be expressed as function of partition function using 2-xiii.

Evaluation of the partition function involves a rigorous mathematical equation which considers occurrence of all microstates a system. Because there can be infinite configurations of microstates realizing a particular set of macroscopic properties, molecular dynamics relies on important assumption given by the ergodic hypothesis, which states that the time average of a property is equal to its ensemble average. The basic idea is that if the system is allowed to evolve in time indefinitely, that system will eventually pass through all possible states. Ensemble average $\langle A \rangle_{ensemble}$ and time average $\langle \boldsymbol{A} \rangle_{\boldsymbol{time}}$ of any macroscopic property A are given below:

$$\langle A \rangle_{ensemble} = \int \int \, dp^N \, dr^N A(p^N, r^N) \cdot \Omega(p^N, r^N) \qquad \textbf{2-xiv}$$

$$\langle \boldsymbol{A} \rangle_{\boldsymbol{time}} = \lim_{t \to \tau} \frac{\mathbf{1}}{\boldsymbol{\tau}} \int_{\mathbf{0}}^{\boldsymbol{\tau}} \boldsymbol{A}\left(\boldsymbol{p}^{\boldsymbol{N}}(\boldsymbol{t}), \boldsymbol{r}^{\boldsymbol{N}}(\boldsymbol{t})\right) \boldsymbol{dt} = \frac{\mathbf{1}}{\boldsymbol{T}} \sum_{\boldsymbol{t}=\mathbf{0}}^{\boldsymbol{t}=\boldsymbol{T}} \boldsymbol{A}(\boldsymbol{p}^{\boldsymbol{N}}, \boldsymbol{r}^{\boldsymbol{N}}) \qquad \textbf{2-xv}$$

where *r* is the position of atoms, *p* is momentum of atoms, and *T* is simulation time of the molecular dynamics calculation. Correlations for physical properties are developed from classical thermodynamics and statistical mechanics. For example, the equation for pressure is developed using the virial equation as shown below:

$$P = \frac{N k_B T}{V} + \frac{1}{6V} \left[\sum_{P_1=1}^{N} \sum_{j \neq i}^{N} r_{ij} f_{ij} \right] \qquad \textbf{2-xvi}$$

where *N* is the number of molecules in the system, k_B is Boltzmann's constant, *V* and *T* are volume and temperature of the computational domain, and f_{ij} is force between molecules i and j. Based on the type of ensemble chosen, certain macroscopic properties are conserved computationally throughout the simulation using thermostats and barostats.

The measurement of macroscopic properties becomes meaningful only after it goes through a sufficient number of microstates such that the ensemble properties do not change significantly. This process is known as equilibration. The system under study must undergo equilibration before simulation of experimental conditions in order to have an accurate understanding of the experimentally observed phenomena. Equilibration takes place in two stages: the equilibration cycle and the production cycle. In the equilibration cycle, $\langle A \rangle_{ensemble} \neq \langle \mathrm{A} \rangle_{\mathrm{time}}$; therefore the standard deviation of macroscopic properties is significant. Once the standard deviation becomes negligible, the ensemble average of these properties does not vary much with changing microstate, which implies that $\langle A \rangle_{ensemble} = \langle \mathrm{A} \rangle_{\mathrm{time}}$. Hence, the system under observation realizes the macroscopic properties that were present before the start of the simulation.

The types of ensembles chosen in molecular dynamics are:

- **Microcanonical Ensemble (**NVE). The thermodynamic state of a system is characterized by a fixed number of atoms N, volume V, and energy E.
- **Canonical Ensemble (**NVT). This is a collection of all systems whose thermodynamic state is characterized by a fixed number of atoms N, volume V, and temperature T.
- **Isobaric-Isothermal Ensemble (**NPT). This ensemble is characterized by a fixed number of atoms N, pressure P, and temperature T.
- **Grand Canonical Ensemble (**μVT). The thermodynamic state for this ensemble is characterized by a fixed chemical potential μ, volume V, and temperature, T.

2.3.2 Thermostats and barostats in molecular dynamics

In order to control the temperature and pressure of the system, the time-integration technique is modified to damp the velocity and position changes. Common thermostats and barostats used in

molecular dynamics are the Berendsen thermostat, Berendsen barostat, Nosé-Hoover thermostat, and Parrinello-Rahman barostats. The Berendsen thermostat and barostat and Nosé-Hoover thermostat are used in this work for equilibration of hemicellulose systems. In the Berendsen thermostat, temperature control is established by using the relationship between the kinetic energy with temperature and incorporating an additional term in Newton's second law of motion to scale the updated velocity in equation 2-ix. Pressure is controlled by a scaling parameter that is developed by relating the change in pressure to isothermal compressibility, which is applied to updated position in equation 2-x and simulation box length [11]. The choice of damping constant directly affects the dynamics of the system; therefore, the choice of thermostat/barostat should not alter the behavior of system to a large extent and should be effective in maintaining the ensemble average.

2.4 Force field

A force field contains detailed descriptions of the functional form and parameters required to calculate the potential energy of the system in molecular dynamics calculations. Phenomena captured by molecular dynamics mainly depend on accuracy of predicting behavior of the system on a molecular level. The energy potential is designed based on structural properties of the particles and their interactions with neighboring particles. Various potentials are designed to study the behavior of biological macromolecules, polymers, coarse-grained molecules, adsorption chemistry, chemical reactions of inorganic, organic compounds, etc. thus, they are essential to understand many phenomena significant in designing industrial processes.

Total energy of the system is a function of the bonded interactions and non-bonded interactions:

2-xvii

$$E_{system} = E_{BI} + E_{NBI}$$

where E_{BI} and E_{NBI} are energies due to bonded interactions and non-bonded interactions, respectively, which are functions of positions of the atoms. Bonded interactions refer to potential energy of the molecule that is stored in bonds, angles, and dihedrals. Non-bonded interactions include van der Waals forces, columbic interactions, hydrogen bonding, and other physical forces of attraction. There are specific terms in the potential that account for a characteristic behavior in a particular phenomenon. Transferability of the functional form and parameters is an important measure of the effectiveness of a force field; i.e., the potential should be able to provide similar results for related molecules rather than having to revise the parameters for an individual set of molecules. The force field can be modified by improvising the functional form, by addition of terms, and/or calibration of parameters.

2.4.1 Bonded interactions

The most common bonded interactions observed within molecules are due to bond stretching, angle bending, and dihedral angle change due to rotation around bonds.

- *Bond-stretching term*: Bond-stretching energy varies as a function of the square of displacement from reference bond length. Vibrations in molecules exhibit the properties of both harmonic potential and Morse potential [12]. The bond-stretching term can be expressed conventionally as:

$$U_{bonds}(l) = \frac{k}{2}(l - l_0)^2[1 - k_1(l - l_0) - k_2(l - l_0)^2 \dots] \qquad \textbf{2-xviii}$$

  where k, k_1, k_2 are predefined force constants, l_0 is the reference bond length, and l is the equilibrium bond length. Inclusion of higher terms ensures more closeness to the Morse potential.

- *Angle-bending term:* A similar functional form of energy is applicable for bending of angles. Distortion of an angle from equilibrium requires less energy than stretching or compression of bonds, therefore force constants are smaller.

  Energy due to angle bending can be conventionally expressed as:

$$U_{angle}(\theta) = \frac{ka}{2}(\theta - \theta_0)^2[1 - ka_1(\theta - \theta_0) - ka_2(\theta - \theta_0)^2 \dots] \qquad \textbf{2-xix}$$

  Higher-order terms are included not only to improve the accuracy but also to account for highly strained molecules [12].

- *Torsional-angle term:* Bond-stretching and angle-bending terms are known as "hard" degrees of freedom; i.e., a substantial energy should be supplied in order to bring these changes. Most variation in structure is due to complex interplay between torsional and non-bonded contributions. Torsional changes occur due to rotation of groups around bonds. Energy contribution due to variation in torsional angles can be expressed conventionally as:

$$U_{torsions}(\omega) = \sum_{n=0}^{N} \frac{v_n}{2}[1 + \cos(n\omega - \nu)] \qquad \textbf{2-xx}$$

  where ω is torsion angle, v_n is barrier height that indicates the easiness with which a bond can rotate, *n* is multiplicity (the minimum number of points in the function when the bond is rotated through 360º), and ν is phase factor, which is the minimum value of torsion angle [12].

2.4.2 Non-bonded interactions:

Non-bonded interactions capture the intermolecular and intramolecular physical forces of attraction among the molecules. Intramolecular forces are calculated between pairs of atoms separated by at least three bonds.

- *Lennard-Jones Potential:* Potential that evaluates the effect of van der Waals forces of interaction between a pair of atoms.

$$u_{LJ}(r_{ij}) = \sum_{i=1} \sum_{j \neq i}^{N} 4\varepsilon_{ij} \left[\left(\frac{\sigma_{ij}}{r_{ij}} \right)^{12} - \left(\frac{\sigma_{ij}}{r_{ij}} \right)^{6} \right] \quad \textbf{2-xxi}$$

where ε is the depth of the potential well, σ is the finite distance at which the inter-particle potential is zero, and *r* is the distance between the particles.

- *Coulombic Potential:* Potential developed to capture effects of electrostatic forces of attraction between a pair of atoms.

$$u_c(r_{ij}) = \sum_{i=1} \sum_{j \neq i}^{N} \frac{q_i q_j}{4\pi\varepsilon_0 r_{ij}} \quad \textbf{2-xxii}$$

where q_i, q_j are partial charges of pairs of atoms *i* and *j*, r_{ij} is separation distance between them, and $k_e = \frac{1}{4\pi\varepsilon_0}$ is the Coulomb constant, equal to 8.88×10^9 N•m^{2}C^{-2}.

CHAPTER 3: REACTIVE FORCE FIELD: REAXFF POTENTIAL

Reactive potentials are designed to capture reaction events taking place in system under observation with evolution of time. The first potential for understanding the progression of a reaction based on bond order was developed by J. Tersoff [14]. It was developed by modeling potential energy of the system as a function of a three-body interaction of each atom with the neighboring atoms summed over for all atoms in a system. This method did not accurately describe the reaction phenomena observed because only local neighbor environment was considered to be contributing to interactions affecting a reaction event. However, the description of dynamics of a reactive system as a function of bond order turned out to be an effective approach to bridge the gap between quantum-mechanics calculations and classical molecular-dynamics approach.

Many empirical models such as VALBOND [14], REBO [15], and AIREBO [16] potentials were developed to overcome the shortcomings of the Tersoff potential, but none of these models considered the role of long-range interactions as a factor in occurrence of a reaction phenomenon. RMDff is another reactive force field that uses bond order but is based on established equilibrium force field [17]. The ReaxFF force field developed by van Duin et al. [13] is a deterministic model that has effectively described the reaction phenomena by factoring in long-range interactions and polarizability effects along with neighbor-atom interactions as function of bond order [18].

Bond order is defined as the number of bonds existing between two atoms which generally is a whole number. In the ReaxFF potential, bond orders are considered to be continuous functions of interatomic positions, and all bonded interactions are a function of bond orders. The continuous nature of bond order allows the calculation to capture how the molecule is transitioning during a

reaction. The energy of a system is directly dependent on a reaction event; i.e., bond scission or bond formation. With time integration performed on positions and velocities of atoms, reactive events undergone by the system can also be tracked with evolution of time.

In order to ensure transferability, each element has unique force field parameters. For example, the elemental carbon is described by a set of force field parameters and there is no distinction between sp^2 and sp^3 carbon. This feature ensures that the force field can be applicable for a wide range of systems undergoing different types of reactions [18].

The potential energy of the system is described as shown below:

$$E_{system} = E_{bond} + E_{atom} + E_{lp} + E_{angle} + E_{co-angle} + E_{hb} + E_{tors} + E_{co-tors} + E_{coulomb} + E_{vdWaal} \quad \textbf{3-i}$$

where $E_{coulomb}, E_{vdWaals}$ are the non-bonded interaction terms and the remaining terms represent bonded interactions which is a function of bond orders. Detailed description of each terms can be found in the supporting information of reference [12]. These terms have been modified to capture different types of reactions. For example, the force field describing combustion will have different parameters for elemental C than the force field describing adsorption of molecules on carbon material. In other words, the force field is not general but rather is equipped to capture characteristic phenomena particular to a reaction. The bonded interactions used to describe a reaction are bond energy, valence angle energy, torsional energy, lone pair energy, overcoordination (when bond order is greater than valency of atom), and energy correction for aromatic stability. Under favorable temperature and pressure conditions, contribution of each of the bonded and non-bonded terms will lead to a particular reaction path.

Bond order is a function of interatomic separation between atoms. It contains characteristics of single, double, and triple bond.

$$BO_{ij} = BO_{ij}^{\sigma} + BO_{ij}^{\pi} + BO_{ij}^{\pi\pi} \qquad \textbf{3-iii}$$

$$BO_{ij} = \exp\left[p_{bo1}\left(\frac{r_{ij}}{r_0^{\sigma}} \right)^{p_{bo2}} \right] + \exp\left[p_{bo3}\left(\frac{r_{ij}}{r_0^{\sigma}} \right)^{p_{bo4}} \right] + \exp\left[p_{bo5}\left(\frac{r_{ij}}{r_0^{\pi\pi}} \right)^{p_{bo6}} \right] \qquad \textbf{3-iii}$$

In a state of transition, the bond order will contain partial characteristics of two types of bonds which can quantitatively set apart various kinds of reaction mechanism.

Partial charge of each atom, required for evaluation of coulombic potential, is calculated based on the QEq equilibration method. The QEq algorithm assigns partial charges to atoms such that electrostatic energy of the system is minimized, keeping the system's total charge constant [19].

CHAPTER 4: SIMULATION DETAILS

Xylan pyrolysis is a complex process to control due to amorphous nature of polymer. As structure of xylan is not known, the pyrolysis reaction simulations are first bring carried out by simulating pyrolysis reaction of β-D-xylopyranose to determine all reaction pathways involving the monomer xylan. The reactive molecular dynamics and quantum chemistry calculations were carried out in the henry2 High Performance Computing system at NC State University.

4.1 Reactive Molecular Dynamics calculations

The Reactive Molecular Dynamics calculations were carried out using LAMMPS [20] software developed by Sandia National Laboratory with an extended ReaxFF force field developed by van Duin *et al*. [21] The β-D-xylopyranose pyrolysis has been studied to deduce reaction pathways and determine kinetics of each reaction with two types of systems given below:

1. "Isolated β-D-xylopyranose system" – A single xylose molecule with 10 argon atoms in a simulation box.
2. "Large molecular system" - 50 β-D-xylopyranose molecules with argon atoms in a simulation box.

The reactions taking place in these two types of system would reveal favorability of reactions taking in bulk phase and the effects of other molecules, even though they may not participate in the elementary reactions directly.

Design of simulation box

The system of β-D-xylopyranose and argon molecules are generated in a periodic simulation box using Packmol [22], which is minimized using conjugate gradient algorithm [23]

in LAMMPS. The density of the simulation box is calculated based on the pyroprobe sample taken for Py-GCxGC/ToFMS experiments.

Experimental conditions

- Weight of the sample = 0.5 mg
- Inert flow rate (He) = 70 ml/minute
- Radius of sample tube = 1.25 mm
- Length of sample tube = 25 mm
- Molecular weight of sample (β-D-xylopyranose) = 150.13 g/mol

$\Rightarrow$ Volume of sample tube = $\frac{\pi}{4}(1.25mm)^2(25mm) = 1.22768 \times 10^{-7} m^3$

$\Rightarrow$ Density of sample = Weight of the sample taken /Volume of sample tube

$$= \frac{\frac{0{\cdot}5\times10^{-3}\,g}{150.13\frac{g}{\text{mol}}} \times 6.023\times10^{23}\frac{molecules}{\text{mol}}}{1.22768\times10^{-7}\cdot10^{30}\,\text{Å}^3}$$

$$= 1.6343 \times 10^{-5} \text{ molecules/ Å}^3$$

Isolated β-D-xylopyranose reaction simulation box

$\Rightarrow$ Volume of box with one β-D-xylopyranose molecule = $\frac{1 \text{ molecule}}{1.6343\times10^{-5}\text{molecules/ Å}^3}$

$$= 61202.6 \text{ Å}^3$$

$\Rightarrow$ Length of cubic simulation box = 39.4 Å

Large molecular β-D-xylopyranose reaction simulation box

$\Rightarrow$ Volume of box with 50 β-D-xylopyranose molecules = $\frac{50 \text{ molecules}}{1{\cdot}6343\times10^{-5}\text{molecules}/\text{Å}^3}$

$= 3060132 \text{ Å}^3$

$\Rightarrow$ Length of cubic simulation box = 145.2 Å

Equilibration

Equilibration is necessary for establishing similarity between experimental conditions and simulation as discussed in section 2.3. The minimized system is equilibrated as an NPT ensemble at temperatures 523 K, 573 K, 623 K, and 673 K and 1 atm pressure with extended ReaxFF force field [21]. Berendsen thermostat and barostats were used for maintaining the above conditions [11]. The temperature damping constant is 100 fs and the pressure damping constant is 1000 fs. The numerical integration is performed using Velocity-Verlet algorithm with 0.1 fs as timestep for 250 ps, and trajectory of atoms was recorded every 1000 timesteps.

ReaxFF MD calculations

The Reactive Molecular Dynamics calculations are carried out for three different microstates chosen from the trajectory once readiness for the production cycle is attained during the equilibration stage. That conditions allows determination of a statistical average of the kinetic rate constant for elementary reactions obtained from the simulation.

The isolated β-D-xylopyranose system after equilibration undergoes pyrolysis through numerical integration using Velocity-Verlet algorithm, maintaining an NVE ensemble with 0.25 fs as timestep using extended ReaxFF force field [21] until all reactions are completed. Pyrolysis reactions of isolated β-D-xylopyranose are studied in order to determine the temperature range

during which reactions occur. Temperature range in which stable reactions were observed between 1500 K and 2250 K. The large molecular system is equilibrated with Velocity-Verlet algorithm maintaining an NPT ensemble with 0.1 fs as timestep using extended ReaxFF force field [18] in the temperature range obtained from the isolated system until all reactions are completed. Reference [23] recommends, "The increased simulation temperature would be of great help in observing slow and thermodynamically possible reactions at lower temperatures within pico-seconds". As the systems monitored are comprised of molecules with flexible bonds that undergo translational, rotational, torsional, and vibrational motion, reference [24] further recommends that the time step taken should be an order faster than the fastest motion found in the system, making it approximately 1 fs [25]. Therefore a timestep of 0.1 fs seems appropriate in order to record the nuances of bond scission or bond formation, as ReaxFF MD tracking of the bond order change every time [26].

The NPT Reactive Molecular Dynamics calculations are carried out at temperatures 1500 K, 1750 K, 2000 K, and 2250 K using Nosé-Hoover thermostat and barostats [27,28] with temperature damping constant of 10 fs and a pressure damping constant of 350 fs. The reaction completion depends on various factors such as temperature, pressure, and molecular system configuration. The potential energy, kinetic energy, and bond order change in each molecule were recorded over time to measure the energy change during a reaction event. Analysis of bond orders and the trajectory for the simulations is done by using the commercial visualization tool MAPS, which was developed by Scienomics [25].

CHAPTER 5: RESULTS AND DISCUSSION

The temperature effects of β-D-xylopyranose pyrolysis have been investigated by constant temperature ReaxFF MD simulation and Py-GCxGC/TOF MS experiments. Pyrolysis of hemicellulose pyrolysis reactions were hypothesized to follow pericyclic reaction mechanisms. A reaction is considered to be pericyclic when bonds are transferred in a concerted manner within a cyclic transition state. The complexity of the transition state can be a great challenge for determining kinetics of such reactions by Reactive Molecular Dynamics.

Reactive Molecular Dynamics simulations using a ReaxFF force field potentially provides an effective approach to understand this class of reactions, as bond orders between pairs of atoms are tracked with evolution of time that is sensitive to macroscopic properties related to experimental conditions. Bond order change determined at every timestep can describe nuances observed in a pericyclic reaction quantitatively. The relationship of reactive events with respect to time paves a way to estimate kinetic parameters governing the reactions taking place for the system under observation. The reaction pathways are developed based on the bond order analysis of the given system at every picosecond and verified by comparison to covalent radii estimations for pairs of atoms [25].

5.1 Reaction pathways for isolated β-D-xylopyranose pyrolysis

The NVE ReaxFF MD calculations for isolated β-D-xylopyranose pyrolysis have predicted formation of D-xylose, ethenol, ethenediol, formaldehyde, formic acid, glyoxal, dihydroxycyclopropane, and water. The reaction pathways for the formation of these products are as shown in Figure 5.1.

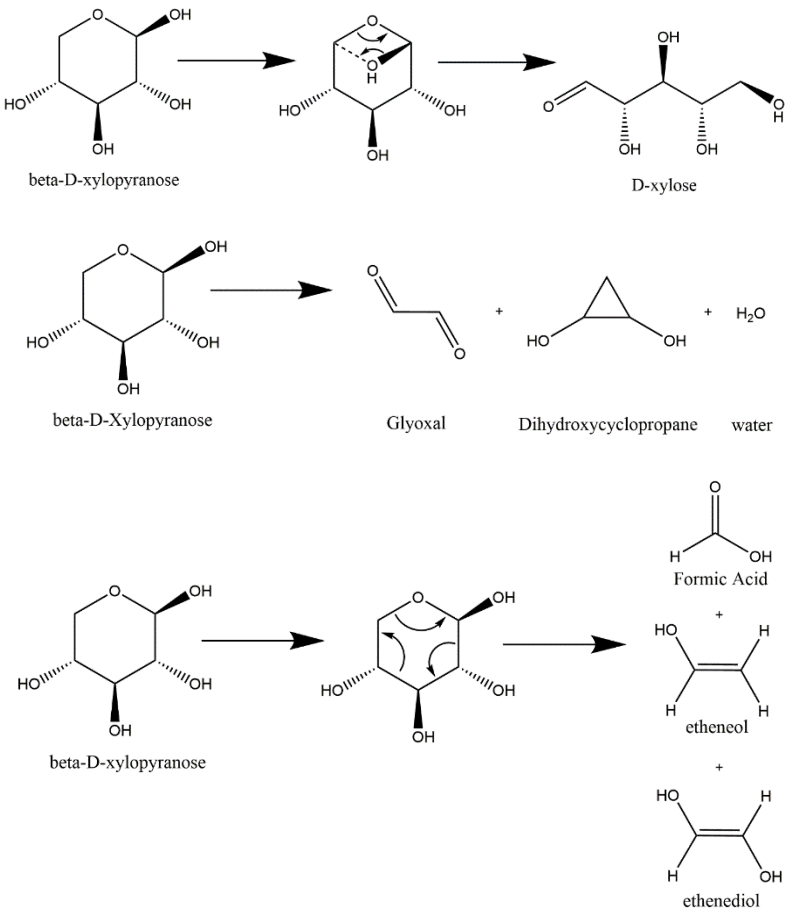

Figure 5.1 Reaction pathways discovered during isolated system NVE ReaxFF MD. Inferred transition structures are developed by analyzing bond information obtained from ReaxFF MD.

The ReaxFF MD calculations with NVE ensemble has uncovered very few reaction pathways, but an approximation of temperature range can be made in which molecules undergo bond scission leading to useful chemical products observed in Py-GCxGC/ToFMS experiment. The above reactions take place between 1500 K – 2250 K.

5.2 Reaction pathways for pyrolysis of the large molecular system

The ReaxFF MD calculations with NPT ensemble performed at 1 atm pressure and 1500 K, 1750 K, 2000 K, and 2250 K has predicted the formation of formic acid, formaldehyde, ethenol,

ethenediol, glyceraldehyde, and other qualitative products through reaction pathways as shown in Figure 5.2.

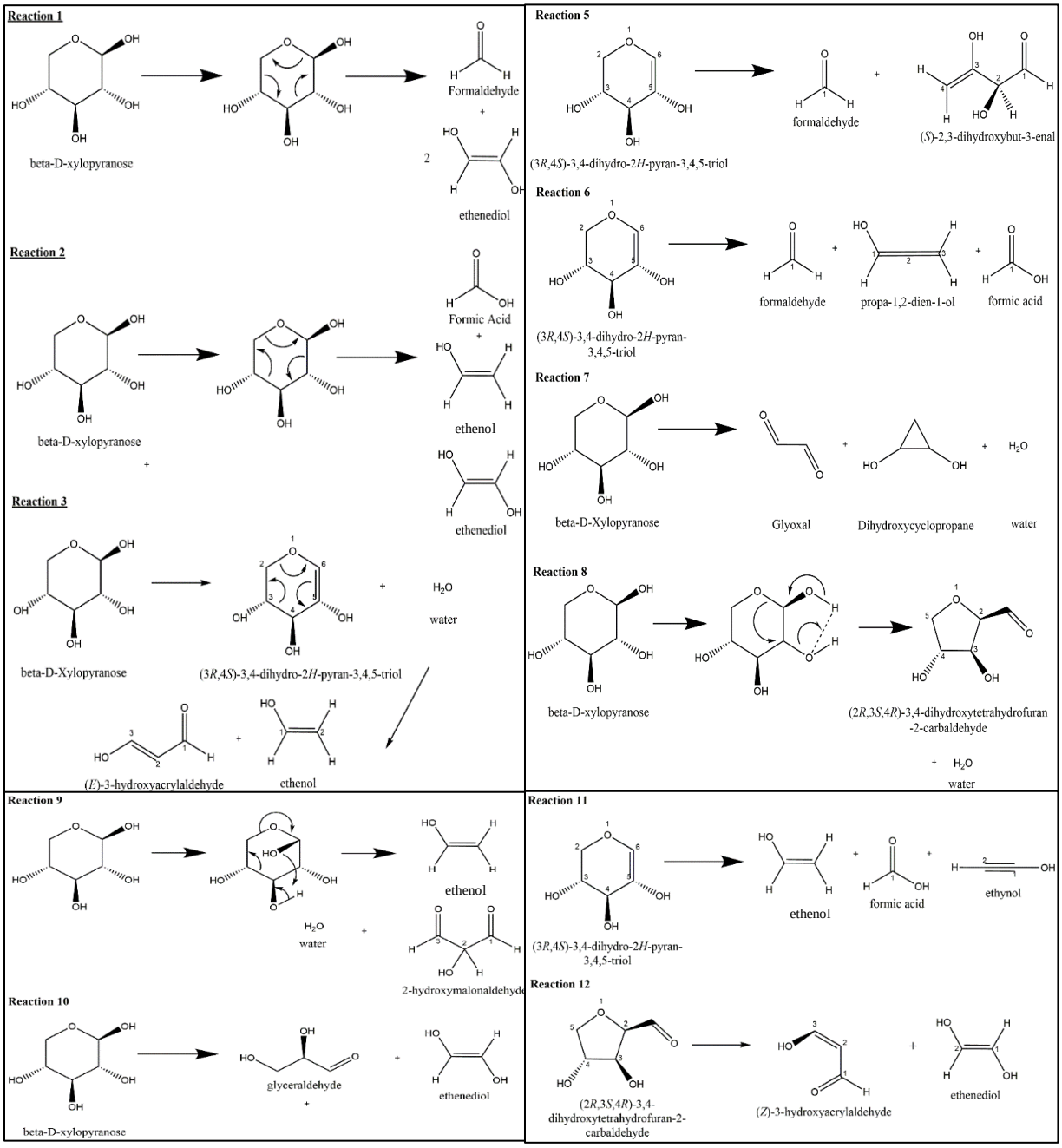

Figure 5.2 Reaction pathways discovered during NPT ReaxFF MD of large molecular system. Inferred transition structures are developed by analyzing bond information obtained from ReaxFF MD using MAPS [29]

5.3 Effect of temperature in reaction pathway selectivity

The trajectories of the system are analyzed to determine species formed at regular intervals of time in order to make qualitative assessment of reactions that govern β-D-xylopyranose pyrolysis.

The following inferences can be drawn from the variation of amount of species with respect to time, as measured at 1500 K, 1750 K, 2000 K and 2250 K:

- The products formed at 1500 K are shown in Figure 5.3: formic acid, formaldehyde, ethenol, ethene-1,2-diol, 2-hydroxymalonaldehyde, and glyceraldehyde. Reactions 1 and 2 are predominant at this temperature, leading to the formation of major products observed. However, glyceraldehyde and 2-hydroxymalonaldehyde were found to be minor products, indicating that reactions 10 and 11 have lower selectivity at the given conditions of simulation. Reactions 10 and 11 are new additions to the reaction pathways that were previously observed isolated-system pyrolysis simulations but the ring-opening reaction of β-D-xylopyranose to form D-xylose was not observed in the large molecular system pyrolysis.
- The products formed at 1750 K are shown in Figure 5.4: formic acid, formaldehyde, ethenol, ethene-1,2-diol, water, (2R,3S,4R)-3,4-dihydroxytetrahydrofuran-2-carbaldehyde (furan derivative), and (Z)-3-hydroxyacrylaldehyde. Reaction 1 and 2 lead to the formation of major products and minor products furan derivative and (Z)-3-hydroxyacrylaldehyde are formed by reactions 8 and 9.
- The products formed at 2000 K are shown in Figure 5.5: formic acid, ethenol, ethene-1,2-diol, water, propa-1,2-dien-1-ol, glyoxal, (3R,4S)-3,4-dihydro-2H-pyran-3,4,5-triol (pyran derivative), and (E)-3-hydroxyacrylaldehyde. Ethene-1,2-diol, ethenol, and formic acid are major products formed as a result of higher selectivity of reaction 1 over other pathways. Minor

products formed are as a result of reaction 3,6 and 7. Glyoxal is one of the products obtained from xylan pyrolysis in Py-GCxGC/TOFMS; this reaction path piques special interest.

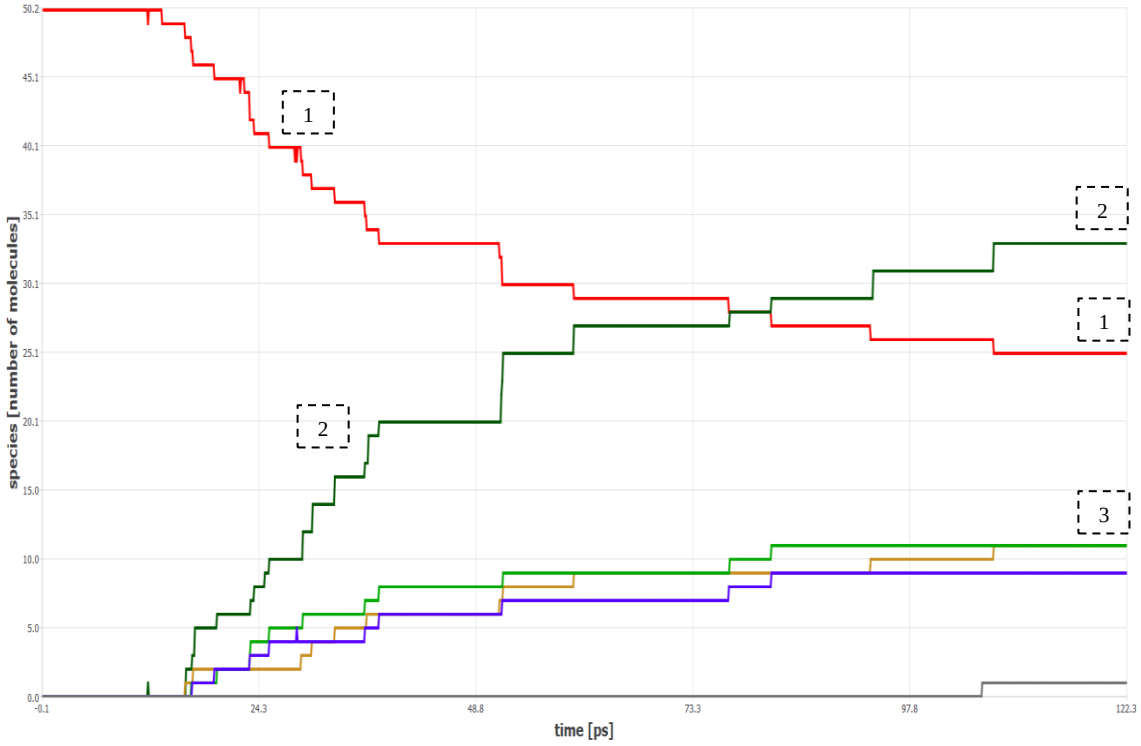

Figure 5.3 (a)

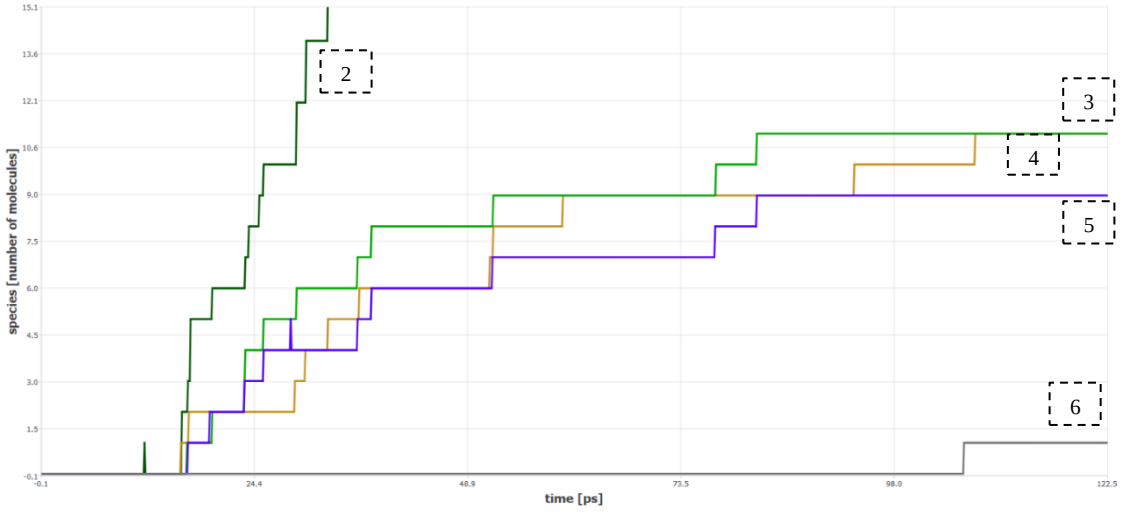

Figure 5.3 (b)

Figure 5.3 Species vs time (ps) for NPT ReaxFF MD for large molecular system at T=1500 K and P= 1 atm (a) All products (b) minor products; Line 1: β-D-xylopyranose, Line 2: ethenediol, Line 3: ethenol, Line 4: formaldehyde, Line 5: formic acid, Line 6: 2-hydroxymalonaldehyde.

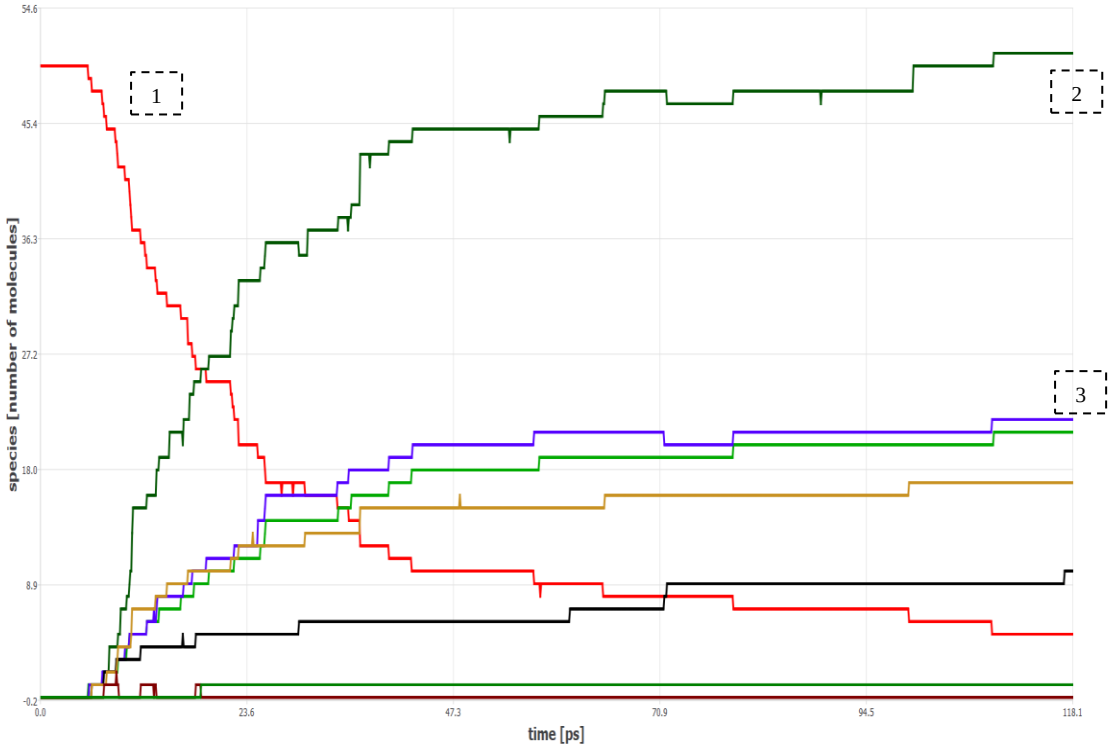

Figure 5.4 (a)

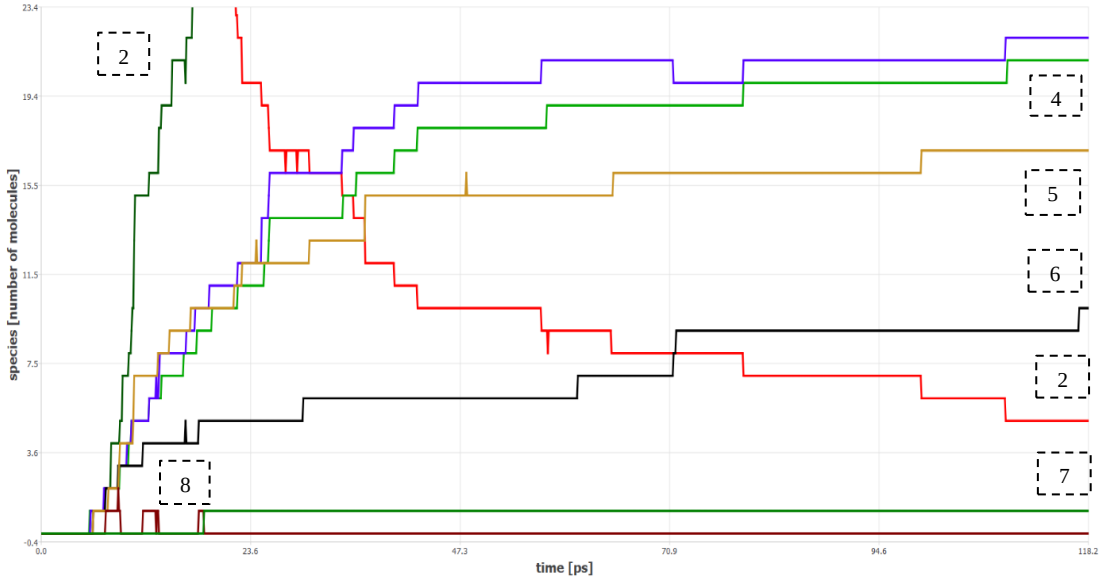

Figure 5.4 (b)

Figure 5.4 Species vs time (ps) for NPT ReaxFF MD of large molecular system at T= 1750 K and P = 1 atm. Line 1: β-D-xylopyranose, Line 2: ethenediol, Line 3: ethenol, Line 4: formic acid, Line 5: formaldehyde, Line 6: water, Line 7: (Z)-3-hydroxyacrylaldehyde, Line 8: (2R,3S,4R)-3,4-dihydroxytetrahydrofuran-2-carbaldehyde.

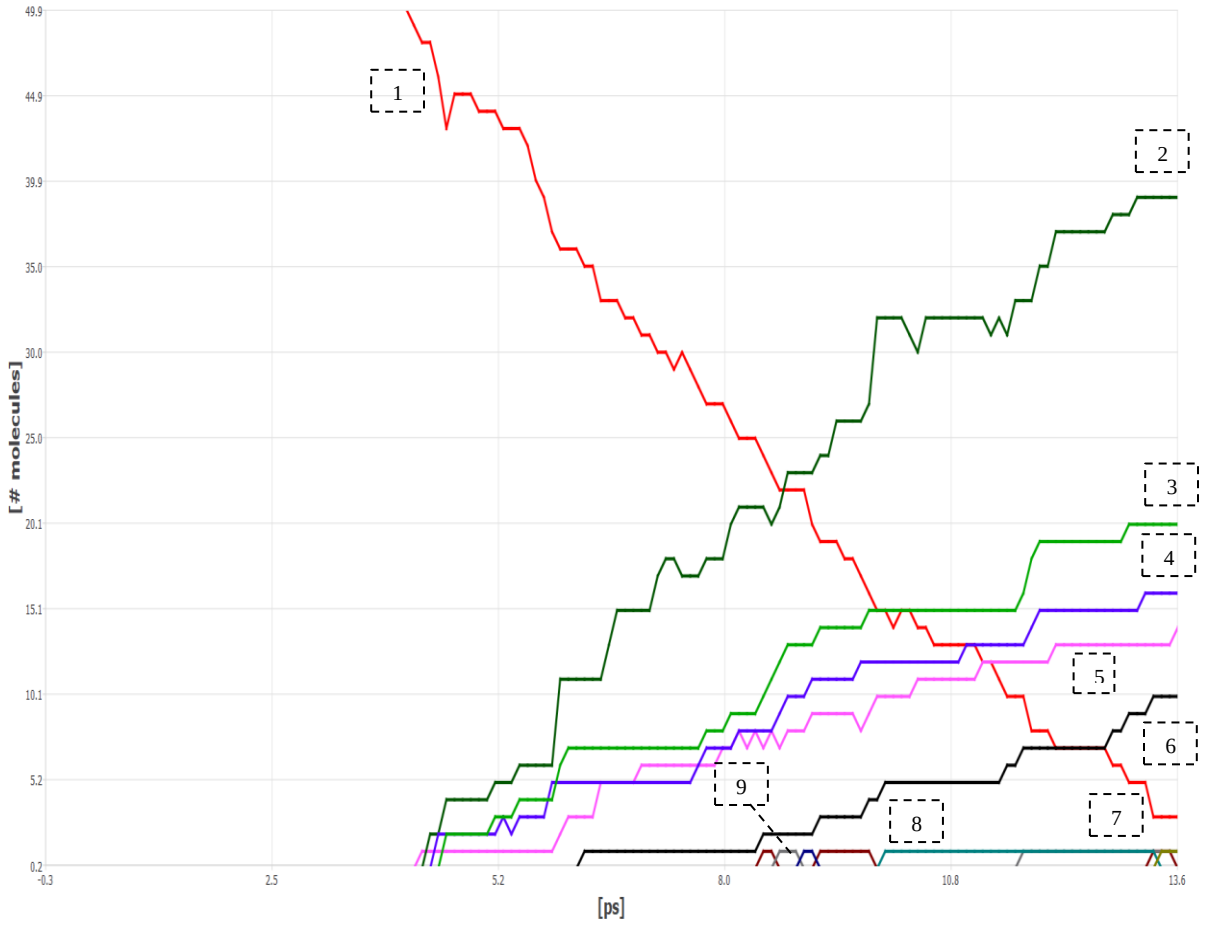

Figure 5.5 Species vs time (ps) for NPT ReaxFF MD of large molecular systems at T= 2000 K and P = 1 atm. Line 1: β-D-xylopyranose, Line 2: ethene-1,2-diol, Line 3: ethenol, Line 4: formic acid, Line 5: water, Line 6: formaldehyde, Line 7: glyoxal, Line 8: (3R,4S)-3,4-dihydro-2H-pyran-3,4,5-triol (pyran derivative), Line 9: (Z) 3-hydroxyacrylaldehyde.

- The products formed at 2250 K are shown in Figure 5.6: formic acid, formaldehyde, ethenol, ethene-1,2-diol, water, glyceraldehyde, (3R,4S)-3,4-dihydro-2H-pyran-3,4,5-triol (pyran derivative), (S)-2,3-dihydroxybut-3-enal, and (Z)-3-hydroxyacrylaldehyde. Ethene-1,2-diol, ethenol, and formic acid are major products formed because reaction 1 and 2 display higher selectivity compared to other pathways. Minor products are formed as a result of reactions 4,5, and 6.
- The reaction pathways driven by dehydration are prominent in NPT ReaxFF MD for large molecular systems at T=1750 K and T= 2000 K leading to formation of molecules with three carbon atoms and molecules with four carbon atoms.
- Increase in temperature of isothermal-isobaric system has unlocked more thermodynamically stable reaction pathways, leading to formation of many enol products and fewer ketones.

5.4 Comparison of product distribution with pyrolysis experiment results

The pyrolysis reactions of β-D-xylopyranose have been measured by Pyroprobe pyrolysis, and reaction products are separated by two-dimensional gas chromatography with TOF mass spectrometry. The product distribution of β-D-xylopyranose pyrolysis was determined as %w/w yield of each product by variation of temperature [26].

In the Py-GCxGC/ToFMS experiment, the β-D-xylopyranose sample is heated at a rate of 1000 ºC/min. As a result, the sample rises almost instantly to the given isotherm temperature at atmospheric pressure, followed by the pyrolysis process. Comparison of product distribution from Py-GCxGC/ToFMS experiment (Figure 5.7) with products obtained from Reactive Molecular Dynamics (Figure 5.8) has provided insights into the pyrolysis mechanism and shortcomings of ReaxFF MD in determination of reaction pathways of all products observed in the experiment.

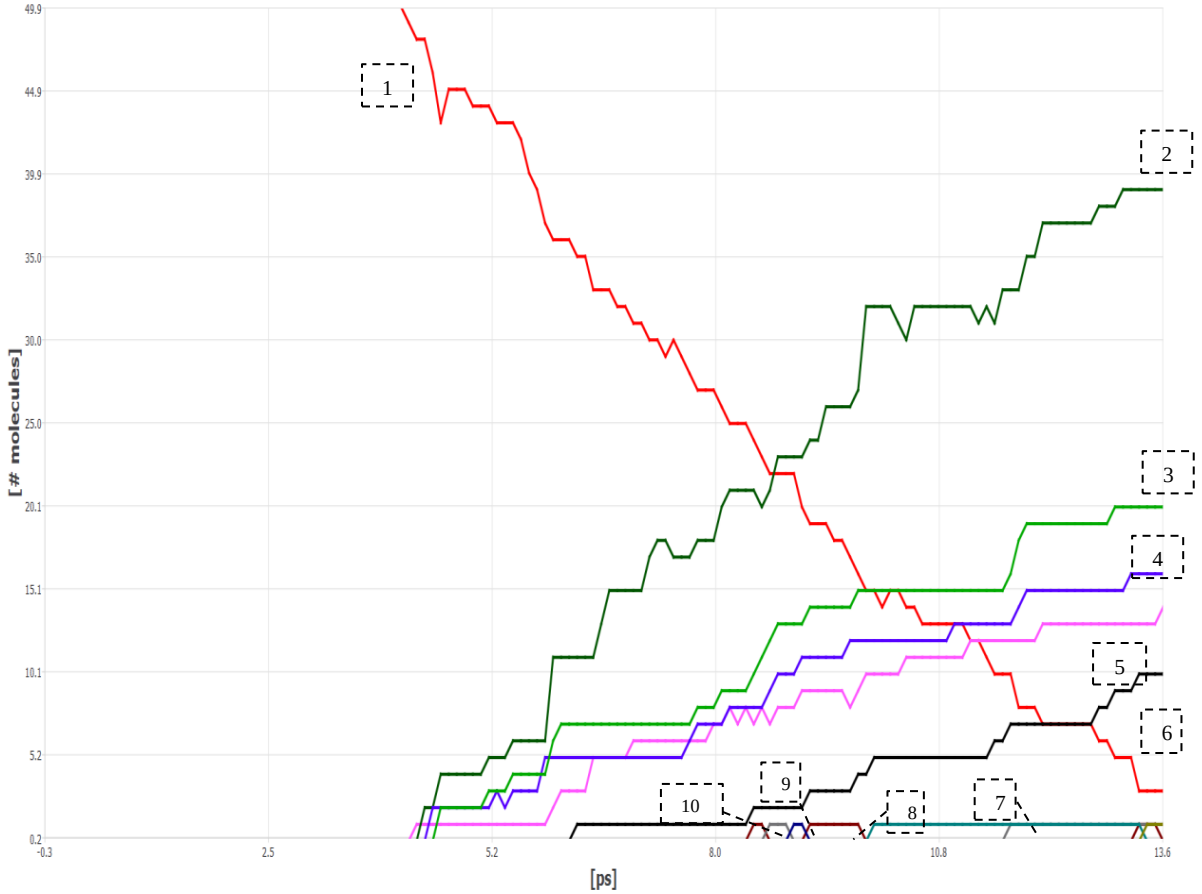

Figure 5.6 Species vs time (ps) for NPT ReaxFF MD at T=2250 K and P = 1 atm.
Line 1: β-D-xylopyranose, Line 2: ethene-1,2-diol, Line 3: ethenol, Line 4: formic acid, line 5: formaldehyde, Line 6: water. Line 7: ethynol, Line 8: (E)-3-hydroxyacrylaldehyde, Line 9: glyoxal, Line 10: dihydroxycyclopropane.

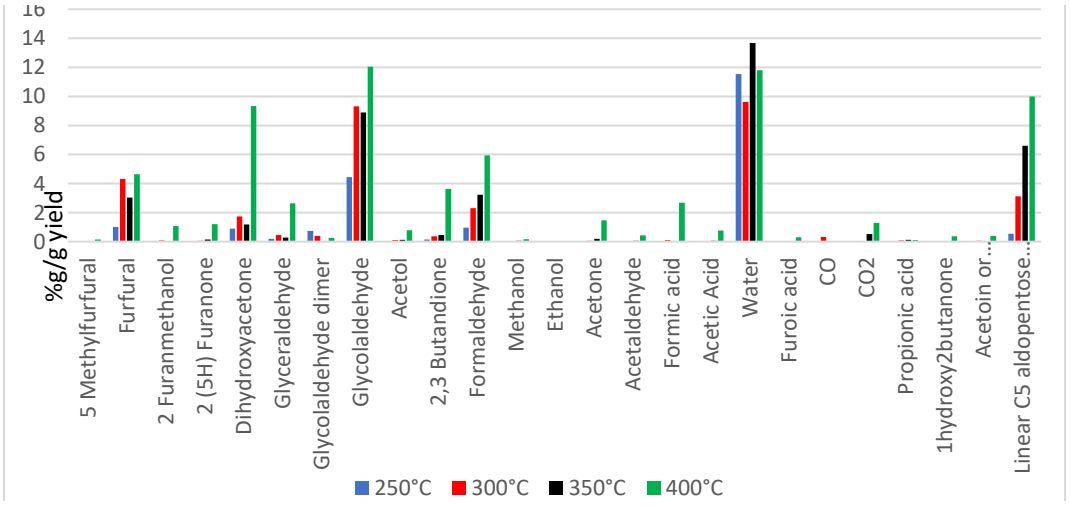

Figure 5.7 β-D-Xylopyranose pyrolysis product distribution from 250ºC-400ºC with 0.5 mg sample size and holding time of 60 s [30].

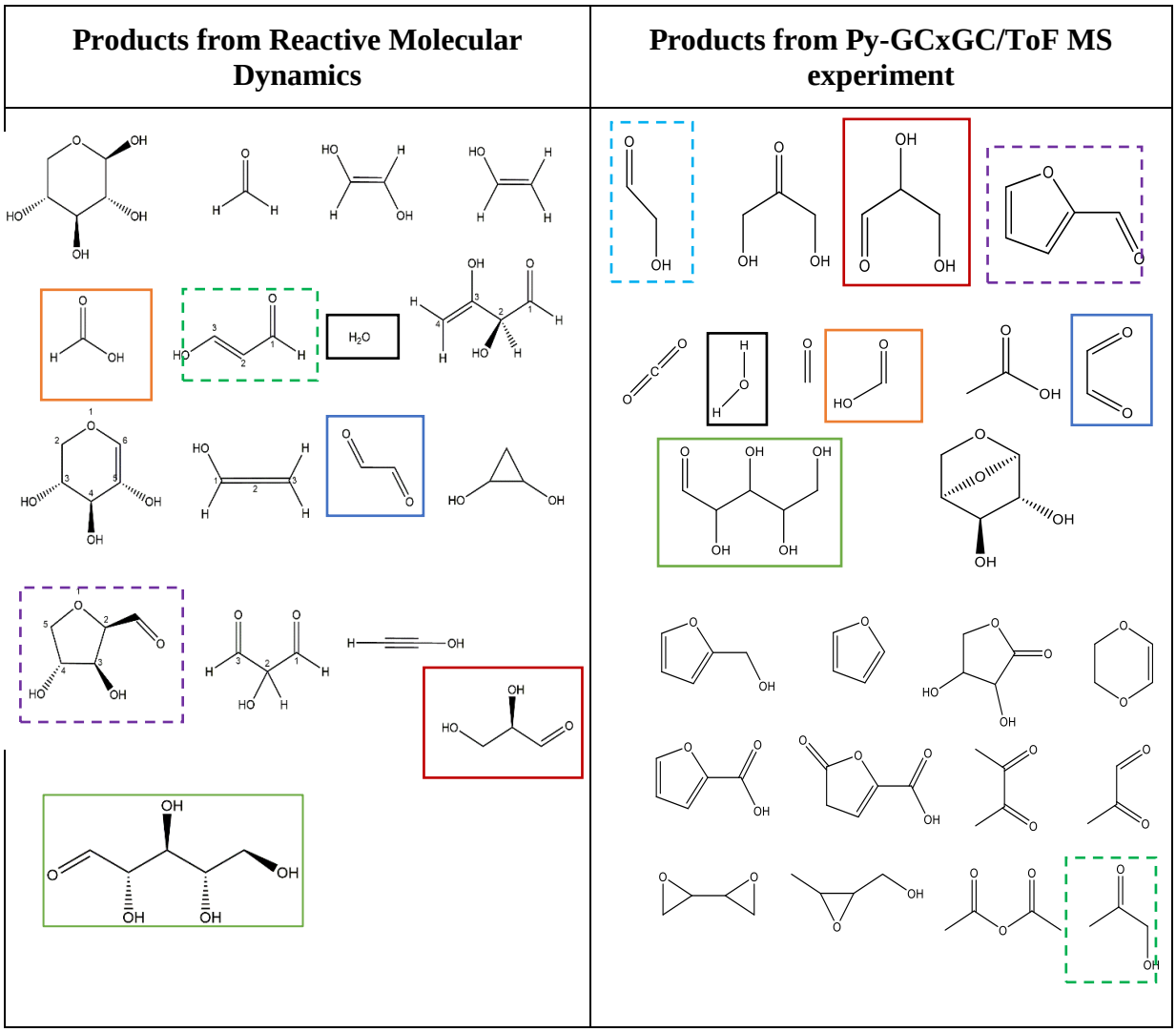

Figure 5.8 Comparison of product distribution between Py-GCxGC/ToFMS experiment and Reactive Molecular dynamics. (The solid lines indicate exact match, and dashed lines indicate structural similarity) [33]

- Reactive Molecular Dynamics (RMD) calculations have identified reaction pathways for qualitative products such as D-xylose, glyceraldehyde, and glyoxal. They have also identified products that are structurally similar to products obtained from the experiments. Ethene-1,2-diol, (E)-3-hydroxyacrylaldehyde, and (2R,3S,4R)-3,4-dihydroxytetrahydrofuran-2-carbaldehyde from RMD are structurally similar to glycolaldehyde, 1-hydroxypropan-2-one, and furfural, respectively.

- The products of pyrolysis experiment contain ketone groups, while the product distribution predicted by Reactive Molecular Dynamics mostly consists of enol products with ketone group product in minor quantities. Ethene-1,2-diol is an enol tautomer of glycolaldehyde, and both are both major products determined from the respective techniques. The dominance of enol products in the ReaxFF MD compared to the experiments might possibly be attributed to phase change that occurs during heating the sample in pyroprobe. During the heating process, an unknown fraction of the β-D-xylopyranose sample melts into the liquid phase and the rest of the sample vaporizes. The keto form of a molecule is known to be more stable in aqueous phase than its enol form; hence it is speculated that products observed in experiment maybe a result of reactions taking place in the liquid xylose phase.
- This speculation can also be supported by comparison of product distribution in Reactive Molecular Dynamics vs pyrolysis experiment. The products containing ketone groups are formed in small quantities compared to the products containing enol groups. As the simulation proceeds, the volume of simulation box dramatically increases indicating the molecules generate a gas phase as time progresses therefore, increasing the selectivity of reaction pathways leading to enol products.
- A reasonable hypothesis is that reaction pathways leading to formation of some of major products are initiated by dehydration reactions. This hypothesis can be supported by lower concentration of water molecules observed in ReaxFF MD simulations and compared to higher yield of water from experiments.
- The products from Reactive Molecular Dynamics calculations are generally chirally hindered. This effect could pose restrictions on reaction pathways, resulting in formation of products that are experimentally observed.

5.5 Analysis of reaction pathways with quantum chemistry

Many of the reaction pathways developed from the simulation of pyrolysis reactions with ReaxFF MD are pericyclic reactions with four-centered and six-centered transition states. Quantum chemistry calculations were performed by McGill [29] using density functional theory (B3LYP/6-31G(d,p)) technique in Gaussian 16 [31] to assess the analysis by ReaxFF MD, which was developed using empirical techniques.

The reaction pathways leading to formation of major products observed in simulations are doubtfully feasible at the given experimental conditions. Berny optimization was performed on the RMD transition structure observed for Reaction 1, the reaction with highest selectivity, which are formic acid, ethenol and ethene-1,2-diol. Based on the transition state search, energies along the coordinate were computed to verify the corresponding product(s) from reactant(s).

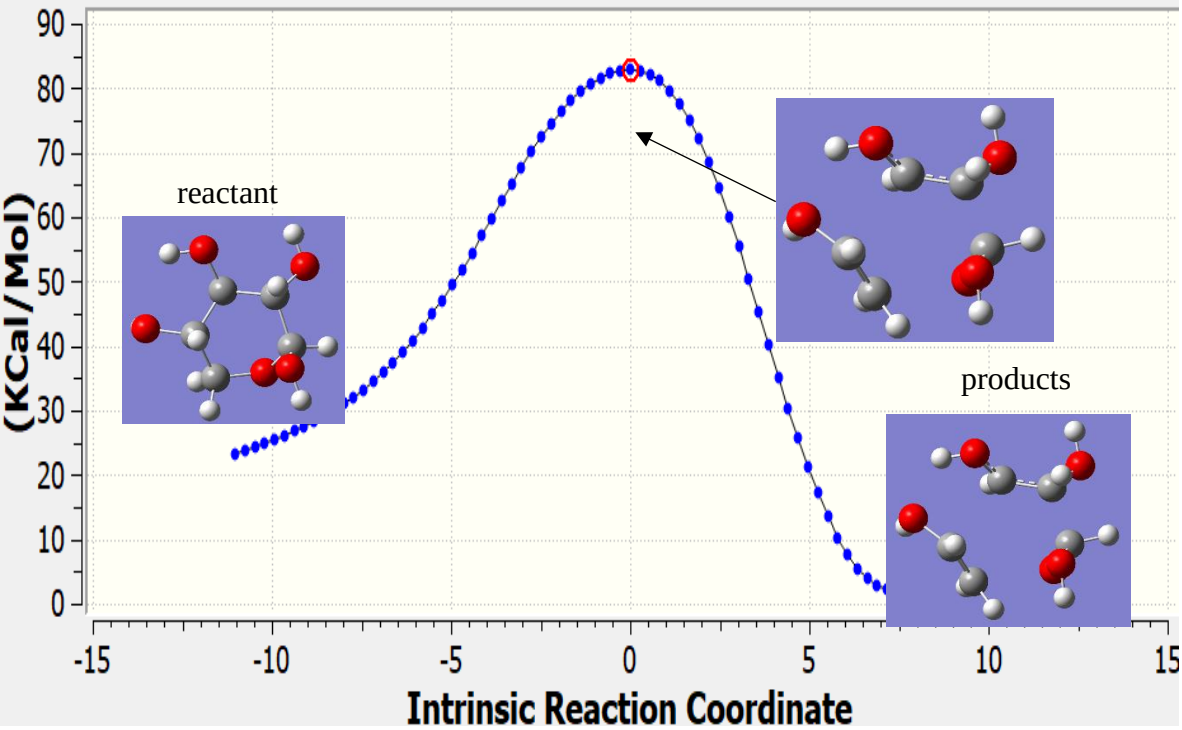

Figure 5.9 Berny transition state optimization of reaction 1, followed by intrinsic reaction coordinate calculation.

From the intrinsic reaction coordinate in Figure 5.9, the reaction pathway is a concerted mechanism leading to formation of products as predicted by ReaxFF MD. It also indicated that this reaction would require at least 61 kcal/mol to cross the energy barrier; therefore, the reaction may not be feasible at the experimental conditions.

Another characteristic reaction pathway predicted by Reactive Molecular Dynamics led to the formation of a furan derivative (reaction 8), this product is particularly interesting due to its structural similarity with furfural. The reaction mechanism is known as a ring-contraction mechanism, which goes through a six-membered transition state as predicted by the Berny optimization technique.

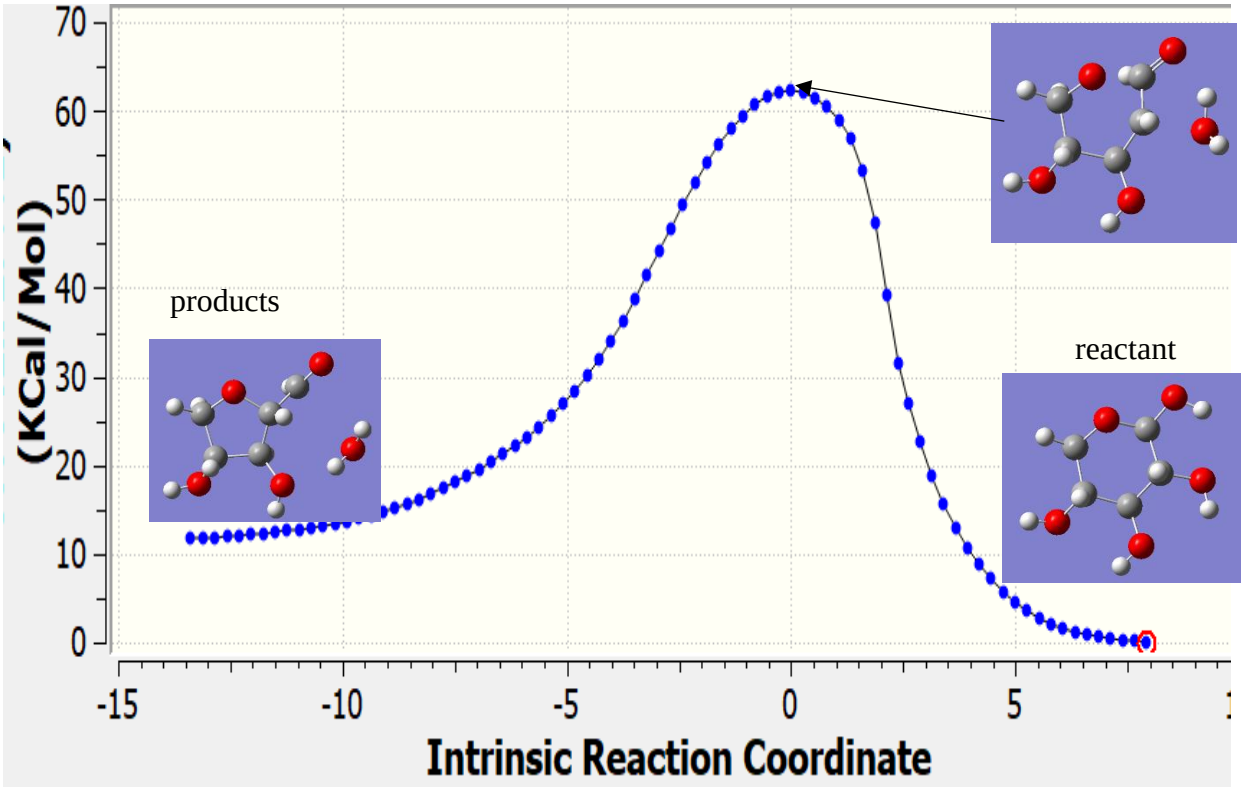

Figure 5.10 Berny transition state optimization for formation of furan derivative followed by intrinsic reaction coordinate calculation by McGill [33].

The quantum chemistry calculations by McGill and Westmoreland [32] have also identified a six-membered concerted mechanism leading to formation of furan derivative with a change in chirality in carbon 1 (containing the HCO group). The intrinsic reaction coordinate for this pathway is shown in Figure 5.10. According to the study of reaction paths for formation of furfural from xylan pyrolysis by McGill and Westmoreland [32], ring contraction of β-D-xylopyranose needs to form (2S,3S,4R)-3,4-dihydroxytetrahydrofuran-2-carbaldehyde as an intermediate product, which would undergo further dehydration to form furfural.

However, ReaxFF MD predicted the formation of its more chirally hindered conformer (2R,3S,4R)-3,4-dihydroxytetrahydrofuran-2-carbaldehyde. Therefore, furfural was not observed in the present Reactive Molecular Dynamics calculations.

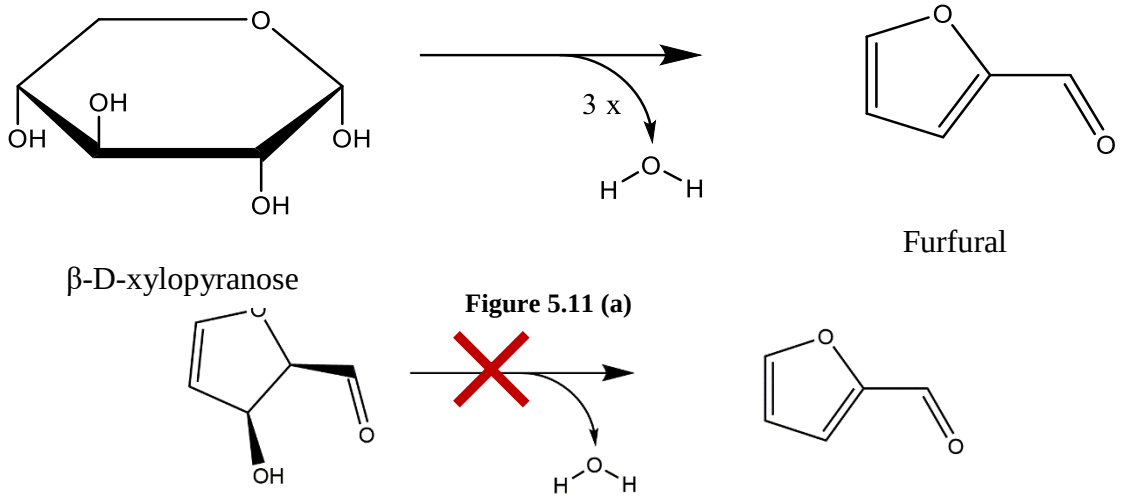

Figure 5.11 (b)

Figure 5.11 (a) Reaction pathway for formation of furfural through ring contraction mechanism (b) forbidden dehydration reaction due to steric hindrance between C1 and C2 for dehydration [32]

CHAPTER 6: CONCLUSIONS AND RECOMMENDATIONS

6.1 Conclusions

The Reactive Molecular Dynamics calculations were performed for simulation of β-D-xylopyranose pyrolysis to understand the reaction pathways governing the process. Products observed in the Py-GCxGC/ToF MS experiment that have been detected in ReaxFF MD calculations are glyceraldehyde, D-xylose, and glyoxal. Ethene-1,2-diol, (E)-3-hydroxyacrylaldehyde, and (2R,3S,4R)-3,4-dihydroxytetrahydrofuran-2-carbaldehyde are also detected in NPT ReaxFF MD calculations that are structurally similar to glycolaldehyde, 1-hydroxypropan-2-one, and furfural, respectively, which are major products that have useful chemical applications.

Reaction pathways developed using Reactive Molecular Dynamics calculations favored reaction paths leading to products with enol groups compared to pathways leading to formation of sterically hindered products with keto group. The experimental product distribution consists of products with ketone groups in higher proportion compared to the products with enol groups. Based on this observation, it can be speculated that the reactions taking place leading to major products in pyrolysis experiment could occur during the heating process when the sample in the solid phase undergoes phase transition resulting a fraction of sample to be in the liquid phase and the rest being in the gas phase. This phase transition could not be seen in simulations, indicating there is a gap in establishing a parallel between experimental conditions and simulation conditions.

From analyzing the nature of the concerted mechanism, we observe from simulations we can infer that the reaction pathways with six-membered transition state occur more frequently compared to concerted reactions with four-membered transition state. The only four-membered transition state pericyclic reaction observed is the ring opening of β-D-xylopyranose to form D-

xylose (reaction 1 in isolated molecule ReaxFF MD NVE simulation). The quantum chemistry calculations reveal that reaction pathways predicted by Reactive Molecular Dynamics have high activation energy; therefore, products generated by these reaction paths are less probable to observe from experiment. Some of the major products observed in simulations are enol tautomers of major products observed in the experiment. Since keto-enol tautomerization is an endothermic reaction, one could speculate that the reaction pathways leading to the formation of keto tautomer of the same product have reasonable activation energies, making the reactions more feasible.

In conclusion, Reactive Molecular Dynamics has proven to be a powerful tool for studying the reaction mechanisms governing pyrolysis process for a given temperature and pressure. Bridging the gap between experimental procedure and simulation technique, higher selectivity of reaction pathways leading to formation of products containing keto groups with reasonable activation can be observed during simulations and ultimately could justify the product distribution obtained from the Py-GCxGC/ToFMS experiments.

6.2 Future work

Reactive Molecular Dynamics has a high potential to determine feasible reaction pathways and chemical kinetics governing pyrolysis of lignocellulosic biomass. One of the many challenges in understanding pyrolysis chemistry is the minimal knowledge of polymer structure of the biomass that is highly sensitive to the source it is taken from. Therefore, determining the structure of beechwood xylan would be invaluable in understanding the reaction pathways in pyrolysis process better.

Experimental results from pyrolysis of xylobiose (a glycosylxylose; that is, D-xylopyranose having a beta-D-xylopyranose residue attached at position 4 via a glycosidic bond), and glucuronic acid in the Westmoreland lab indicate that xylobiose could also be the monomer of beechwood

xylan with a glucuronic acid molecule in the side chain [25]. After optimizing the simulation procedure for β-D-xylopyranose, similar ReaxFF MD calculations can be done for xylobiose and glucuronic acid, comparing the product distribution to pyrolysis experiment results to understand the reaction pathways governing the pyrolysis process. The product distribution of β-D-xylopyranose, xylobiose, and glucuronic acid can be compared with product distribution observed in xylan pyrolysis conducted in Py-GCxGC/ToFMS to confirm the suspicion and develop insights about the polymer chemistry of xylan. Structure determination of xylan and reaction pathways of pyrolysis process for given conditions can be useful in designing reactors to carry out pyrolysis of beechwood xylan.

REFERENCES

[1] G. S. Bala, H-H. Carstensen, K. M. V. Geem, and G. B. Marin, "Measuring Biomass. Fast Pyrolysis Kinetics: State of the Art," *Wiley WIREs Energy Environ*, vol. 8, no. 2, March 2019.

[2] X. Zhou, W. Li, R. Mabon and, L. J. Broadbelt, "A Critical Review on Hemicellulose Pyrolysis," *Special Issue: Pyrolysis for Energy Technologies*, vol. 5, no. 1, pp. 52–79, January 2017.

[3] L. Verlet, "Computer 'Experiments' on Classical Fluids. I. Thermodynamical Properties of Lennard-Jones Molecules," *Physical Review*, pp. 98-103, 1967.

[4] R. E. Wilde and S. Singh, *Statistical Mechanics: Fundamentals and Modern Applications*, New York: John Wiley & Sons, Inc, 1998.

[5] "Theory of Molecular Dynamics Simulations," [Online]. Available: https://embnet.vital-it.ch/MD_tutorial/pages/MD.Part1.html#Verlet [Accessed March 1, 2019].

[6] H. C. Andersen, P. H. Berens, K. R. Wilson and W. C. Swope, "A Computer Simulation Method for the Calculation of Equilibrium Constants for the Formation of Physical Clusters of Molecules: Application to Smaller Water Clusters," *Journal of Chemical Physics*, vol. 76, no. 648, 1982

[7] M. E. Tuckerman, *Statistical Mechanics: Theory and Molecular Simulations*, New York: Oxford University Press, 2010, pp. 99–100.

[8] S. Kim, "Issues on the Choice of a Proper Time Step in Molecular Dynamics," *Physics Procedia*, vol. 53, pp. 60–62, 2014.

[9] J. W. Gibbs, *Elementary Principles in Statistical Mechanics*, New York: Charles Scribner's Sons, 1902.

[10] J. P. M. Postma, W. F. van Gunsteren, A. D. Nola, J. R. Haak, and H. J. C. Berendsen, "Molecular Dynamics with Coupling to an External Bath," *J. Chem. Phys,* vol. 81, no. 3684, 1984.

[11] B. S. D. Frenkel, *Understanding Molecular Simulation: From Algorithms to Applications,* Cambridge, MA: Academic Press, 1996.

[12] S. Dasgupta, F. Lorant, W. A. Goddard and A. C. T. van Duin, "ReaxFF: A Reactive Force Field for Hydrocarbons," *The Journal of Physical Chemistry A,* vol. 105, no. 41, pp 9396–9409, 2001.

[13] J. Tersoff, "New Empirical Approach for the Structure and Energy of Covalent Systems," *Phys. Rev. B,* vol. 37, no. 12, 1988.

[14] Timothy K. Firman, and Clark R. Landis, "Valence Bond Concepts Applied to the Molecular Mechanics Description of Molecular Shapes. 4. Transition Metals with π-Bonds," *J. Am. Chem. Soc.,* 2001, 123 (47), pp 11728–11742.

[15] Donald W. Brenner, Olga A Shenderova, Judith A Harrison, Steven J Stuart, Boris Ni, and Susan B. Sinnott, "A second-generation reactive empirical bond order (REBO) potential energy expression for hydrocarbon," *Journal of Physics: Condensed Matter*, 2002, 14, pp 783-803.

[16] D.W. Brenner, "Emperical potential for hydrocarbons for use in simulating the chemical vapour deposition of diamond films," *Phys Rev B,* vol. 42, pp. 9458-9471, 1990.

[17] K. D. Smith, S. I. Stoliarov, M. R. Nyden, and P. R. Westmoreland, "RMDff: A smoothly transitioning, forcefield-based representation of kinetics for reactive molecular dynamics simulations," *Molecular Simulation,* 2007, 33, pp 361-368.

[18] A. C. T van Duin, "ReaxFF Manual," [Online]. Available: https://www.engr.psu.edu/adri/ReaxffManual.aspx. [Accessed February 20, 2019].

[19] S. A. Pandit, A. C. T. van Duin, A. Y. Grama and H. M. Aktulga, "Parallel Reactive Molecular Dynamics: Numerical Methods and Algorithmic Techniques," *Parallel Computing*, vol. 38, no. 245–259, 2012.

[20] S. Plimpton, "Fast Parallel Algorithms for Short-Range Molecular Dynamics," *J Comp Phys*, vol. 117, pp. 1–19, 1995. https://lammps.sandia.gov/

[21] A. C. T. van Duin. A. Yakovlev and A. M. Kamat, "Molecular Dynamics Simulations of Laser-Induced Incandescence of Soot Using an Extended ReaxFF Reactive Force Field," *J. Phys. Chem. A*, vol. 114, no. 48, pp. 12561–12572, 2010.

[22] R. Andrade, J. M. Martinez, E. G. Birgin and L. Martínez, "PACKMOL: A Package for Building Initial Configurations for Molecular Dynamics Simulations," *J Comput Chem*, vol. 30, no. 13, pp. 2157–2164, 2009.

[23] Z. Wei, Q. Zhao and G Yuan, "A Modified Polak–Ribière–Polyak Conjugate Gradient Algorithm for Nonsmooth Convex Programs," *Journal of Computational and Applied Mathematics*, vol. 225, pp. 86–96, 2014.

[24] X. Liu, J. Li, Z. Wang, B. Kong, X. Gong, X. Yang, W. Lin and L. Guo, "Study of High Density Polyethylene (HDPE) Pyrolysis with Reactive Molecular Dynamics," *Polymer Degradation and Stability*, vol. 104, pp. 62–70, 2014.

[25] A. C. T. van Duin, W. A. Goddard, and K. Chenoweth, "ReaxFF Reactive Force Field for Molecular Dynamics Simulations of Hydrocarbon Oxidation," *J. Phys. Chem. A*, vol. 112, no. 5, pp. 1040–1053, 2008.

[26] N. Shuichi, "A Unified Formulation of the Constant Temperature Molecular Dynamics Methods," *The Journal of Chemical Physics*, vol. 81, no. 1, pp. 511–519, 1984.

[27] W. G. Hoover, "Canonical Dynamics: Equilibrium Phase-Space Distributions," *Physical Review A (General Physics)*, vol. 31, no. 3, pp. 1695–1697, 1985.

[28] S. W. Benson, *Thermochemical Kinetics: Methods for the Estimation of Thermochemical Data and Rate Parameters*, New York: Wiley; 2nd Edition, 1976.

[29] "Material Processes and Simulations (MAPS)", Scienomics, [Online]. Available: https://scienomics.com.

[30] A. Bose, personal correspondence, November 2018.

[31] M. J. Frisch, G. W. Trucks, H. B. Schlegel, G. E. Scuseria, M. A. Robb, J. R. Cheeseman, G. Scalmani, V. Barone, G. A. Petersson, H. Nakatsuji, X. Li, M. Caricato, A. V. Marenich, J. Bloino, B. G. Janesko, R. Gomperts, B. Mennucci, H. P. Hratchian, J. V. Ortiz, A. F. Izmaylov, J. L. Sonnenberg, D. Williams-Young, F. Ding, F. Lipparini, F. Egidi, J. Goings, B. Peng, A. Petrone, T. Henderson, D. Ranasinghe, V. G. Zakrzewski, J. Gao, N. Rega, G. Zheng, W. Liang, M. Hada, M. Ehara, K. Toyota, R. Fukuda, J. Hasegawa, M. Ishida, T. Nakajima, Y. Honda, O. Kitao, H. Nakai, T. Vreven, K. Throssell, J. A. Montgomery, Jr., J. E. Peralta, F. Ogliaro, M. J. Bearpark, J. J. Heyd, E. N. Brothers, K. N. Kudin, V. N. Staroverov, T. A. Keith, R. Kobayashi, J. Normand, K. Raghavachari, A. P. Rendell, J. C. Burant, S. S. Iyengar, J. Tomasi, M. Cossi, J. M. Millam, M. Klene, C. Adamo, R. Cammi, J. W. Ochterski, R. L. Martin, K. Morokuma, O. Farkas, J. B. Foresman, and D. J. Fox, *Gaussian 16, Revision B.01*, Gaussian, Inc., Wallingford CT, 2016.

[32] C. McGill, "Mechanism Development for the Generation of Furfural in Xylose Pyrolysis," in 2017 AIChE Annual Meeting, Minneapolis, 2017, paper 174g.

[33] C. McGill, personal correspondence, 20 March 2019.

APPENDICES

The Reactive molecular dynamics calculations performed on LAMMPS using ReaxFF force field were analyzed using MAPS software. MAPS software is used for visualization of trajectory, determining the species count as a function of time, species life span, and reads log file generated by LAMMPS to plot potential energy, kinetic energy, pressure, volume, etc. By comparing the variation of species as a function of time measured at different temperature simulations one can determine reaction pathway selectivity with increase in temperature. Appendix 1 provides species count as a function of time in the NPT RMD of large molecular system at 1500 K and 1 atm pressure. Appendix 2 provides the LAMMPS script necessary for carrying out ReaxFF NPT molecular dynamics. A separate script needs to be written for equilibration which would depend on the system that is studied when the user wants to repeat the calculations or perform NPT ReaxFF molecular dynamics calculations.

Appendix 1. Number of simulated molecules of major species as functions of simulated time (ps) for NPT ReaxFF for T=1500 K and P=1 atm (Figure 5.3).

Time [ps]	β-D-xylopyranose / [number of molecules]	Ethene-1,2-diol / [number of molecules]	formaldehyde / [number of molecules]	ethenol / [number of molecules]	Formic acid / [number of molecules]	2-hydroxymal-onaldehyde / [number of molecules]
0	50	0	0	0	0	0
0.1	50	0	0	0	0	0
0.2	50	0	0	0	0	0
0.3	50	0	0	0	0	0
0.4	50	0	0	0	0	0
0.5	50	0	0	0	0	0
0.6	50	0	0	0	0	0
0.7	50	0	0	0	0	0
0.8	50	0	0	0	0	0
0.9	50	0	0	0	0	0
1	50	0	0	0	0	0
1.1	50	0	0	0	0	0
1.2	50	0	0	0	0	0
1.3	50	0	0	0	0	0
1.4	50	0	0	0	0	0
1.5	50	0	0	0	0	0
1.6	50	0	0	0	0	0
1.7	50	0	0	0	0	0
1.8	50	0	0	0	0	0
1.9	50	0	0	0	0	0
2	50	0	0	0	0	0
2.1	50	0	0	0	0	0
2.2	50	0	0	0	0	0
2.3	50	0	0	0	0	0
2.4	50	0	0	0	0	0
2.5	50	0	0	0	0	0
2.6	50	0	0	0	0	0
2.7	50	0	0	0	0	0
2.8	50	0	0	0	0	0
2.9	50	0	0	0	0	0
3	50	0	0	0	0	0
3.1	50	0	0	0	0	0
3.2	50	0	0	0	0	0
3.3	50	0	0	0	0	0
3.4	50	0	0	0	0	0

3.5	50	0	0	0	0	0
3.6	50	0	0	0	0	0
3.7	50	0	0	0	0	0
3.8	50	0	0	0	0	0
3.9	50	0	0	0	0	0
4	50	0	0	0	0	0
4.1	50	0	0	0	0	0
4.2	50	0	0	0	0	0
4.3	50	0	0	0	0	0
4.4	50	0	0	0	0	0
4.5	50	0	0	0	0	0
4.6	50	0	0	0	0	0
4.7	50	0	0	0	0	0
4.8	50	0	0	0	0	0
4.9	50	0	0	0	0	0
5	50	0	0	0	0	0
5.1	50	0	0	0	0	0
5.2	50	0	0	0	0	0
5.3	50	0	0	0	0	0
5.4	50	0	0	0	0	0
5.5	50	0	0	0	0	0
5.6	50	0	0	0	0	0
5.7	50	0	0	0	0	0
5.8	50	0	0	0	0	0
5.9	50	0	0	0	0	0
6	50	0	0	0	0	0
6.1	50	0	0	0	0	0
6.2	50	0	0	0	0	0
6.3	50	0	0	0	0	0
6.4	50	0	0	0	0	0
6.5	50	0	0	0	0	0
6.6	50	0	0	0	0	0
6.7	50	0	0	0	0	0
6.8	50	0	0	0	0	0
6.9	50	0	0	0	0	0
7	50	0	0	0	0	0
7.1	50	0	0	0	0	0
7.2	50	0	0	0	0	0
7.3	50	0	0	0	0	0
7.4	50	0	0	0	0	0
7.5	50	0	0	0	0	0
7.6	50	0	0	0	0	0
7.7	50	0	0	0	0	0

7.8	50	0	0	0	0	0
7.9	50	0	0	0	0	0
8	50	0	0	0	0	0
8.1	50	0	0	0	0	0
8.2	50	0	0	0	0	0
8.3	50	0	0	0	0	0
8.4	50	0	0	0	0	0
8.5	50	0	0	0	0	0
8.6	50	0	0	0	0	0
8.7	50	0	0	0	0	0
8.8	50	0	0	0	0	0
8.9	50	0	0	0	0	0
9	50	0	0	0	0	0
9.1	50	0	0	0	0	0
9.2	50	0	0	0	0	0
9.3	50	0	0	0	0	0
9.4	50	0	0	0	0	0
9.5	50	0	0	0	0	0
9.6	50	0	0	0	0	0
9.7	50	0	0	0	0	0
9.8	50	0	0	0	0	0
9.9	50	0	0	0	0	0
10	50	0	0	0	0	0
10.1	50	0	0	0	0	0
10.2	50	0	0	0	0	0
10.3	50	0	0	0	0	0
10.4	50	0	0	0	0	0
10.5	50	0	0	0	0	0
10.6	50	0	0	0	0	0
10.7	50	0	0	0	0	0
10.8	50	0	0	0	0	0
10.9	50	0	0	0	0	0
11	50	0	0	0	0	0
11.1	50	0	0	0	0	0
11.2	50	0	0	0	0	0
11.3	50	0	0	0	0	0
11.4	50	0	0	0	0	0
11.5	50	0	0	0	0	0
11.6	50	0	0	0	0	0
11.7	50	0	0	0	0	0
11.8	49	1	0	0	0	0
11.9	50	0	0	0	0	0
12	50	0	0	0	0	0

12.1	50	0	0	0	0	0
12.2	50	0	0	0	0	0
12.3	50	0	0	0	0	0
12.4	50	0	0	0	0	0
12.5	50	0	0	0	0	0
12.6	50	0	0	0	0	0
12.7	50	0	0	0	0	0
12.8	50	0	0	0	0	0
12.9	50	0	0	0	0	0
13	50	0	0	0	0	0
13.1	50	0	0	0	0	0
13.2	50	0	0	0	0	0
13.3	50	0	0	0	0	0
13.4	49	0	0	0	0	0
13.5	49	0	0	0	0	0
13.6	49	0	0	0	0	0
13.7	49	0	0	0	0	0
13.8	49	0	0	0	0	0
13.9	49	0	0	0	0	0
14	49	0	0	0	0	0
14.1	49	0	0	0	0	0
14.2	49	0	0	0	0	0
14.3	49	0	0	0	0	0
14.4	49	0	0	0	0	0
14.5	49	0	0	0	0	0
14.6	49	0	0	0	0	0
14.7	49	0	0	0	0	0
14.8	49	0	0	0	0	0
14.9	49	0	0	0	0	0
15	49	0	0	0	0	0
15.1	49	0	0	0	0	0
15.2	49	0	0	0	0	0
15.3	49	0	0	0	0	0
15.4	49	0	0	0	0	0
15.5	49	0	0	0	0	0
15.6	49	0	0	0	0	0
15.7	49	0	0	0	0	0
15.8	49	0	0	0	0	0
15.9	49	0	0	0	0	0
16	48	0	1	0	0	0
16.1	48	2	1	0	0	0
16.2	48	2	1	0	0	0
16.3	48	2	1	0	0	0

16.4	48	2	1	0	0	0
16.5	48	2	1	0	0	0
16.6	48	2	1	0	0	0
16.7	47	2	1	1	0	0
16.8	47	3	1	1	1	0
16.9	46	3	2	1	1	0
17	46	3	2	1	1	0
17.1	46	5	2	1	1	0
17.2	46	5	2	1	1	0
17.3	46	5	2	1	1	0
17.4	46	5	2	1	1	0
17.5	46	5	2	1	1	0
17.6	46	5	2	1	1	0
17.7	46	5	2	1	1	0
17.8	46	5	2	1	1	0
17.9	46	5	2	1	1	0
18	46	5	2	1	1	0
18.1	46	5	2	1	1	0
18.2	46	5	2	1	1	0
18.3	46	5	2	1	1	0
18.4	46	5	2	1	1	0
18.5	46	5	2	1	1	0
18.6	46	5	2	1	1	0
18.7	46	5	2	1	1	0
18.8	46	5	2	1	1	0
18.9	46	5	2	1	1	0
19	46	5	2	1	1	0
19.1	46	5	2	1	1	0
19.2	46	5	2	1	1	0
19.3	45	5	2	1	2	0
19.4	45	5	2	1	2	0
19.5	45	5	2	1	2	0
19.6	45	6	2	2	2	0
19.7	45	6	2	2	2	0
19.8	45	6	2	2	2	0
19.9	45	6	2	2	2	0
20	45	6	2	2	2	0
20.1	45	6	2	2	2	0
20.2	45	6	2	2	2	0
20.3	45	6	2	2	2	0
20.4	45	6	2	2	2	0
20.5	45	6	2	2	2	0
20.6	45	6	2	2	2	0

20.7	45	6	2	2	2	0
20.8	45	6	2	2	2	0
20.9	45	6	2	2	2	0
21	45	6	2	2	2	0
21.1	45	6	2	2	2	0
21.2	45	6	2	2	2	0
21.3	45	6	2	2	2	0
21.4	45	6	2	2	2	0
21.5	45	6	2	2	2	0
21.6	45	6	2	2	2	0
21.7	45	6	2	2	2	0
21.8	45	6	2	2	2	0
21.9	45	6	2	2	2	0
22	45	6	2	2	2	0
22.1	45	6	2	2	2	0
22.2	44	6	2	2	2	0
22.3	45	6	2	2	2	0
22.4	45	6	2	2	2	0
22.5	45	6	2	2	2	0
22.6	45	6	2	2	2	0
22.7	44	6	2	2	2	0
22.8	44	6	2	2	2	0
22.9	44	6	2	2	2	0
23	44	6	2	2	2	0
23.1	44	6	2	2	2	0
23.2	44	6	2	2	2	0
23.3	42	6	2	3	3	0
23.4	42	7	2	4	3	0
23.5	42	7	2	4	3	0
23.6	42	7	2	4	3	0
23.7	42	7	2	4	3	0
23.8	41	8	2	4	3	0
23.9	41	8	2	4	3	0
24	41	8	2	4	3	0
24.1	41	8	2	4	3	0
24.2	41	8	2	4	3	0
24.3	41	8	2	4	3	0
24.4	41	8	2	4	3	0
24.5	41	8	2	4	3	0
24.6	41	8	2	4	3	0
24.7	41	8	2	4	3	0
24.8	41	8	2	4	3	0
24.9	41	8	2	4	3	0

25	41	9	2	4	3	0
25.1	41	9	2	4	3	0
25.2	41	9	2	4	3	0
25.3	41	9	2	4	3	0
25.4	41	9	2	4	3	0
25.5	40	10	2	5	4	0
25.6	40	10	2	5	4	0
25.7	40	10	2	5	4	0
25.8	40	10	2	5	4	0
25.9	40	10	2	5	4	0
26	40	10	2	5	4	0
26.1	40	10	2	5	4	0
26.2	40	10	2	5	4	0
26.3	40	10	2	5	4	0
26.4	40	10	2	5	4	0
26.5	40	10	2	5	4	0
26.6	40	10	2	5	4	0
26.7	40	10	2	5	4	0
26.8	40	10	2	5	4	0
26.9	40	10	2	5	4	0
27	40	10	2	5	4	0
27.1	40	10	2	5	4	0
27.2	40	10	2	5	4	0
27.3	40	10	2	5	4	0
27.4	40	10	2	5	4	0
27.5	40	10	2	5	4	0
27.6	40	10	2	5	4	0
27.7	40	10	2	5	4	0
27.8	40	10	2	5	4	0
27.9	40	10	2	5	4	0
28	40	10	2	5	4	0
28.1	40	10	2	5	4	0
28.2	40	10	2	5	4	0
28.3	40	10	2	5	4	0
28.4	39	10	2	5	4	0
28.5	40	10	2	5	4	0
28.6	39	10	2	5	5	0
28.7	40	10	2	5	4	0
28.8	40	10	2	5	4	0
28.9	40	10	2	5	4	0
29	40	10	2	5	4	0
29.1	39	10	3	5	4	0
29.2	39	10	3	5	4	0

29.3	38	12	3	6	4	0
29.4	38	12	3	6	4	0
29.5	38	12	3	6	4	0
29.6	38	12	3	6	4	0
29.7	38	12	3	6	4	0
29.8	38	12	3	6	4	0
29.9	38	12	3	6	4	0
30	38	12	3	6	4	0
30.1	38	12	3	6	4	0
30.2	38	12	3	6	4	0
30.3	37	12	4	6	4	0
30.4	37	14	4	6	4	0
30.5	37	14	4	6	4	0
30.6	37	14	4	6	4	0
30.7	37	14	4	6	4	0
30.8	37	14	4	6	4	0
30.9	37	14	4	6	4	0
31	37	14	4	6	4	0
31.1	37	14	4	6	4	0
31.2	37	14	4	6	4	0
31.3	37	14	4	6	4	0
31.4	37	14	4	6	4	0
31.5	37	14	4	6	4	0
31.6	37	14	4	6	4	0
31.7	37	14	4	6	4	0
31.8	37	14	4	6	4	0
31.9	37	14	4	6	4	0
32	37	14	4	6	4	0
32.1	37	14	4	6	4	0
32.2	37	14	4	6	4	0
32.3	37	14	4	6	4	0
32.4	37	14	4	6	4	0
32.5	37	14	4	6	4	0
32.6	37	14	4	6	4	0
32.7	37	14	4	6	4	0
32.8	37	14	4	6	4	0
32.9	36	16	5	6	4	0
33	36	16	5	6	4	0
33.1	36	16	5	6	4	0
33.2	36	16	5	6	4	0
33.3	36	16	5	6	4	0
33.4	36	16	5	6	4	0
33.5	36	16	5	6	4	0

33.6	36	16	5	6	4	0
33.7	36	16	5	6	4	0
33.8	36	16	5	6	4	0
33.9	36	16	5	6	4	0
34	36	16	5	6	4	0
34.1	36	16	5	6	4	0
34.2	36	16	5	6	4	0
34.3	36	16	5	6	4	0
34.4	36	16	5	6	4	0
34.5	36	16	5	6	4	0
34.6	36	16	5	6	4	0
34.7	36	16	5	6	4	0
34.8	36	16	5	6	4	0
34.9	36	16	5	6	4	0
35	36	16	5	6	4	0
35.1	36	16	5	6	4	0
35.2	36	16	5	6	4	0
35.3	36	16	5	6	4	0
35.4	36	16	5	6	4	0
35.5	36	16	5	6	4	0
35.6	36	16	5	6	4	0
35.7	36	16	5	6	4	0
35.8	36	16	5	6	4	0
35.9	36	16	5	6	4	0
36	36	16	5	6	4	0
36.1	36	16	5	6	4	0
36.2	36	16	5	6	4	0
36.3	35	17	5	7	5	0
36.4	35	17	5	7	5	0
36.5	34	17	6	7	5	0
36.6	34	17	6	7	5	0
36.7	34	19	6	7	5	0
36.8	34	19	6	7	5	0
36.9	34	19	6	7	5	0
37	34	19	6	7	5	0
37.1	34	19	6	7	5	0
37.2	34	19	6	7	5	0
37.3	34	19	6	7	5	0
37.4	34	19	6	7	5	0
37.5	34	19	6	7	5	0
37.6	34	19	6	7	5	0
37.7	34	19	6	7	5	0
37.8	34	19	6	7	5	0

37.9	33	20	6	8	6	0
38	33	20	6	8	6	0
38.1	33	20	6	8	6	0
38.2	33	20	6	8	6	0
38.3	33	20	6	8	6	0
38.4	33	20	6	8	6	0
38.5	33	20	6	8	6	0
38.6	33	20	6	8	6	0
38.7	33	20	6	8	6	0
38.8	33	20	6	8	6	0
38.9	33	20	6	8	6	0
39	33	20	6	8	6	0
39.1	33	20	6	8	6	0
39.2	33	20	6	8	6	0
39.3	33	20	6	8	6	0
39.4	33	20	6	8	6	0
39.5	33	20	6	8	6	0
39.6	33	20	6	8	6	0
39.7	33	20	6	8	6	0
39.8	33	20	6	8	6	0
39.9	33	20	6	8	6	0
40	33	20	6	8	6	0
40.1	33	20	6	8	6	0
40.2	33	20	6	8	6	0
40.3	33	20	6	8	6	0
40.4	33	20	6	8	6	0
40.5	33	20	6	8	6	0
40.6	33	20	6	8	6	0
40.7	33	20	6	8	6	0
40.8	33	20	6	8	6	0
40.9	33	20	6	8	6	0
41	33	20	6	8	6	0
41.1	33	20	6	8	6	0
41.2	33	20	6	8	6	0
41.3	33	20	6	8	6	0
41.4	33	20	6	8	6	0
41.5	33	20	6	8	6	0
41.6	33	20	6	8	6	0
41.7	33	20	6	8	6	0
41.8	33	20	6	8	6	0
41.9	33	20	6	8	6	0
42	33	20	6	8	6	0
42.1	33	20	6	8	6	0

42.2	33	20	6	8	6	0
42.3	33	20	6	8	6	0
42.4	33	20	6	8	6	0
42.5	33	20	6	8	6	0
42.6	33	20	6	8	6	0
42.7	33	20	6	8	6	0
42.8	33	20	6	8	6	0
42.9	33	20	6	8	6	0
43	33	20	6	8	6	0
43.1	33	20	6	8	6	0
43.2	33	20	6	8	6	0
43.3	33	20	6	8	6	0
43.4	33	20	6	8	6	0
43.5	33	20	6	8	6	0
43.6	33	20	6	8	6	0
43.7	33	20	6	8	6	0
43.8	33	20	6	8	6	0
43.9	33	20	6	8	6	0
44	33	20	6	8	6	0
44.1	33	20	6	8	6	0
44.2	33	20	6	8	6	0
44.3	33	20	6	8	6	0
44.4	33	20	6	8	6	0
44.5	33	20	6	8	6	0
44.6	33	20	6	8	6	0
44.7	33	20	6	8	6	0
44.8	33	20	6	8	6	0
44.9	33	20	6	8	6	0
45	33	20	6	8	6	0
45.1	33	20	6	8	6	0
45.2	33	20	6	8	6	0
45.3	33	20	6	8	6	0
45.4	33	20	6	8	6	0
45.5	33	20	6	8	6	0
45.6	33	20	6	8	6	0
45.7	33	20	6	8	6	0
45.8	33	20	6	8	6	0
45.9	33	20	6	8	6	0
46	33	20	6	8	6	0
46.1	33	20	6	8	6	0
46.2	33	20	6	8	6	0
46.3	33	20	6	8	6	0
46.4	33	20	6	8	6	0

46.5	33	20	6	8	6	0
46.6	33	20	6	8	6	0
46.7	33	20	6	8	6	0
46.8	33	20	6	8	6	0
46.9	33	20	6	8	6	0
47	33	20	6	8	6	0
47.1	33	20	6	8	6	0
47.2	33	20	6	8	6	0
47.3	33	20	6	8	6	0
47.4	33	20	6	8	6	0
47.5	33	20	6	8	6	0
47.6	33	20	6	8	6	0
47.7	33	20	6	8	6	0
47.8	33	20	6	8	6	0
47.9	33	20	6	8	6	0
48	33	20	6	8	6	0
48.1	33	20	6	8	6	0
48.2	33	20	6	8	6	0
48.3	33	20	6	8	6	0
48.4	33	20	6	8	6	0
48.5	33	20	6	8	6	0
48.6	33	20	6	8	6	0
48.7	33	20	6	8	6	0
48.8	33	20	6	8	6	0
48.9	33	20	6	8	6	0
49	33	20	6	8	6	0
49.1	33	20	6	8	6	0
49.2	33	20	6	8	6	0
49.3	33	20	6	8	6	0
49.4	33	20	6	8	6	0
49.5	33	20	6	8	6	0
49.6	33	20	6	8	6	0
49.7	33	20	6	8	6	0
49.8	33	20	6	8	6	0
49.9	33	20	6	8	6	0
50	33	20	6	8	6	0
50.1	33	20	6	8	6	0
50.2	33	20	6	8	6	0
50.3	33	20	6	8	6	0
50.4	33	20	6	8	6	0
50.5	33	20	6	8	6	0
50.6	33	20	6	8	6	0
50.7	33	20	6	8	6	0

50.8	33	20	6	8	6	0
50.9	33	20	6	8	6	0
51	33	20	6	8	6	0
51.1	33	20	6	8	6	0
51.2	33	20	6	8	6	0
51.3	33	20	6	8	6	0
51.4	33	20	6	8	6	0
51.5	32	20	7	8	6	0
51.6	32	20	7	8	6	0
51.7	32	22	7	8	6	0
51.8	30	23	7	8	7	0
51.9	30	25	8	9	7	0
52	30	25	8	9	7	0
52.1	30	25	8	9	7	0
52.2	30	25	8	9	7	0
52.3	30	25	8	9	7	0
52.4	30	25	8	9	7	0
52.5	30	25	8	9	7	0
52.6	30	25	8	9	7	0
52.7	30	25	8	9	7	0
52.8	30	25	8	9	7	0
52.9	30	25	8	9	7	0
53	30	25	8	9	7	0
53.1	30	25	8	9	7	0
53.2	30	25	8	9	7	0
53.3	30	25	8	9	7	0
53.4	30	25	8	9	7	0
53.5	30	25	8	9	7	0
53.6	30	25	8	9	7	0
53.7	30	25	8	9	7	0
53.8	30	25	8	9	7	0
53.9	30	25	8	9	7	0
54	30	25	8	9	7	0
54.1	30	25	8	9	7	0
54.2	30	25	8	9	7	0
54.3	30	25	8	9	7	0
54.4	30	25	8	9	7	0
54.5	30	25	8	9	7	0
54.6	30	25	8	9	7	0
54.7	30	25	8	9	7	0
54.8	30	25	8	9	7	0
54.9	30	25	8	9	7	0
55	30	25	8	9	7	0

55.1	30	25	8	9	7	0
55.2	30	25	8	9	7	0
55.3	30	25	8	9	7	0
55.4	30	25	8	9	7	0
55.5	30	25	8	9	7	0
55.6	30	25	8	9	7	0
55.7	30	25	8	9	7	0
55.8	30	25	8	9	7	0
55.9	30	25	8	9	7	0
56	30	25	8	9	7	0
56.1	30	25	8	9	7	0
56.2	30	25	8	9	7	0
56.3	30	25	8	9	7	0
56.4	30	25	8	9	7	0
56.5	30	25	8	9	7	0
56.6	30	25	8	9	7	0
56.7	30	25	8	9	7	0
56.8	30	25	8	9	7	0
56.9	30	25	8	9	7	0
57	30	25	8	9	7	0
57.1	30	25	8	9	7	0
57.2	30	25	8	9	7	0
57.3	30	25	8	9	7	0
57.4	30	25	8	9	7	0
57.5	30	25	8	9	7	0
57.6	30	25	8	9	7	0
57.7	30	25	8	9	7	0
57.8	30	25	8	9	7	0
57.9	30	25	8	9	7	0
58	30	25	8	9	7	0
58.1	30	25	8	9	7	0
58.2	30	25	8	9	7	0
58.3	30	25	8	9	7	0
58.4	30	25	8	9	7	0
58.5	30	25	8	9	7	0
58.6	30	25	8	9	7	0
58.7	30	25	8	9	7	0
58.8	30	25	8	9	7	0
58.9	30	25	8	9	7	0
59	30	25	8	9	7	0
59.1	30	25	8	9	7	0
59.2	30	25	8	9	7	0
59.3	30	25	8	9	7	0

59.4	30	25	8	9	7	0
59.5	30	25	8	9	7	0
59.6	30	25	8	9	7	0
59.7	30	25	8	9	7	0
59.8	30	25	8	9	7	0
59.9	29	27	9	9	7	0
60	29	27	9	9	7	0
60.1	29	27	9	9	7	0
60.2	29	27	9	9	7	0
60.3	29	27	9	9	7	0
60.4	29	27	9	9	7	0
60.5	29	27	9	9	7	0
60.6	29	27	9	9	7	0
60.7	29	27	9	9	7	0
60.8	29	27	9	9	7	0
60.9	29	27	9	9	7	0
61	29	27	9	9	7	0
61.1	29	27	9	9	7	0
61.2	29	27	9	9	7	0
61.3	29	27	9	9	7	0
61.4	29	27	9	9	7	0
61.5	29	27	9	9	7	0
61.6	29	27	9	9	7	0
61.7	29	27	9	9	7	0
61.8	29	27	9	9	7	0
61.9	29	27	9	9	7	0
62	29	27	9	9	7	0
62.1	29	27	9	9	7	0
62.2	29	27	9	9	7	0
62.3	29	27	9	9	7	0
62.4	29	27	9	9	7	0
62.5	29	27	9	9	7	0
62.6	29	27	9	9	7	0
62.7	29	27	9	9	7	0
62.8	29	27	9	9	7	0
62.9	29	27	9	9	7	0
63	29	27	9	9	7	0
63.1	29	27	9	9	7	0
63.2	29	27	9	9	7	0
63.3	29	27	9	9	7	0
63.4	29	27	9	9	7	0
63.5	29	27	9	9	7	0
63.6	29	27	9	9	7	0

63.7	29	27	9	9	7	0
63.8	29	27	9	9	7	0
63.9	29	27	9	9	7	0
64	29	27	9	9	7	0
64.1	29	27	9	9	7	0
64.2	29	27	9	9	7	0
64.3	29	27	9	9	7	0
64.4	29	27	9	9	7	0
64.5	29	27	9	9	7	0
64.6	29	27	9	9	7	0
64.7	29	27	9	9	7	0
64.8	29	27	9	9	7	0
64.9	29	27	9	9	7	0
65	29	27	9	9	7	0
65.1	29	27	9	9	7	0
65.2	29	27	9	9	7	0
65.3	29	27	9	9	7	0
65.4	29	27	9	9	7	0
65.5	29	27	9	9	7	0
65.6	29	27	9	9	7	0
65.7	29	27	9	9	7	0
65.8	29	27	9	9	7	0
65.9	29	27	9	9	7	0
66	29	27	9	9	7	0
66.1	29	27	9	9	7	0
66.2	29	27	9	9	7	0
66.3	29	27	9	9	7	0
66.4	29	27	9	9	7	0
66.5	29	27	9	9	7	0
66.6	29	27	9	9	7	0
66.7	29	27	9	9	7	0
66.8	29	27	9	9	7	0
66.9	29	27	9	9	7	0
67	29	27	9	9	7	0
67.1	29	27	9	9	7	0
67.2	29	27	9	9	7	0
67.3	29	27	9	9	7	0
67.4	29	27	9	9	7	0
67.5	29	27	9	9	7	0
67.6	29	27	9	9	7	0
67.7	29	27	9	9	7	0
67.8	29	27	9	9	7	0
67.9	29	27	9	9	7	0

68	29	27	9	9	7	0
68.1	29	27	9	9	7	0
68.2	29	27	9	9	7	0
68.3	29	27	9	9	7	0
68.4	29	27	9	9	7	0
68.5	29	27	9	9	7	0
68.6	29	27	9	9	7	0
68.7	29	27	9	9	7	0
68.8	29	27	9	9	7	0
68.9	29	27	9	9	7	0
69	29	27	9	9	7	0
69.1	29	27	9	9	7	0
69.2	29	27	9	9	7	0
69.3	29	27	9	9	7	0
69.4	29	27	9	9	7	0
69.5	29	27	9	9	7	0
69.6	29	27	9	9	7	0
69.7	29	27	9	9	7	0
69.8	29	27	9	9	7	0
69.9	29	27	9	9	7	0
70	29	27	9	9	7	0
70.1	29	27	9	9	7	0
70.2	29	27	9	9	7	0
70.3	29	27	9	9	7	0
70.4	29	27	9	9	7	0
70.5	29	27	9	9	7	0
70.6	29	27	9	9	7	0
70.7	29	27	9	9	7	0
70.8	29	27	9	9	7	0
70.9	29	27	9	9	7	0
71	29	27	9	9	7	0
71.1	29	27	9	9	7	0
71.2	29	27	9	9	7	0
71.3	29	27	9	9	7	0
71.4	29	27	9	9	7	0
71.5	29	27	9	9	7	0
71.6	29	27	9	9	7	0
71.7	29	27	9	9	7	0
71.8	29	27	9	9	7	0
71.9	29	27	9	9	7	0
72	29	27	9	9	7	0
72.1	29	27	9	9	7	0
72.2	29	27	9	9	7	0

72.3	29	27	9	9	7	0
72.4	29	27	9	9	7	0
72.5	29	27	9	9	7	0
72.6	29	27	9	9	7	0
72.7	29	27	9	9	7	0
72.8	29	27	9	9	7	0
72.9	29	27	9	9	7	0
73	29	27	9	9	7	0
73.1	29	27	9	9	7	0
73.2	29	27	9	9	7	0
73.3	29	27	9	9	7	0
73.4	29	27	9	9	7	0
73.5	29	27	9	9	7	0
73.6	29	27	9	9	7	0
73.7	29	27	9	9	7	0
73.8	29	27	9	9	7	0
73.9	29	27	9	9	7	0
74	29	27	9	9	7	0
74.1	29	27	9	9	7	0
74.2	29	27	9	9	7	0
74.3	29	27	9	9	7	0
74.4	29	27	9	9	7	0
74.5	29	27	9	9	7	0
74.6	29	27	9	9	7	0
74.7	29	27	9	9	7	0
74.8	29	27	9	9	7	0
74.9	29	27	9	9	7	0
75	29	27	9	9	7	0
75.1	29	27	9	9	7	0
75.2	29	27	9	9	7	0
75.3	29	27	9	9	7	0
75.4	29	27	9	9	7	0
75.5	29	27	9	9	7	0
75.6	29	27	9	9	7	0
75.7	29	27	9	9	7	0
75.8	29	27	9	9	7	0
75.9	29	27	9	9	7	0
76	29	27	9	9	7	0
76.1	29	27	9	9	7	0
76.2	29	27	9	9	7	0
76.3	29	27	9	9	7	0
76.4	29	27	9	9	7	0
76.5	29	27	9	9	7	0

76.6	29	27	9	9	7	0
76.7	29	27	9	9	7	0
76.8	29	27	9	9	7	0
76.9	29	27	9	9	7	0
77	29	27	9	9	7	0
77.1	29	27	9	9	7	0
77.2	29	27	9	9	7	0
77.3	29	27	9	9	7	0
77.4	28	27	9	9	8	0
77.5	28	28	9	10	8	0
77.6	28	28	9	10	8	0
77.7	28	28	9	10	8	0
77.8	28	28	9	10	8	0
77.9	28	28	9	10	8	0
78	28	28	9	10	8	0
78.1	28	28	9	10	8	0
78.2	28	28	9	10	8	0
78.3	28	28	9	10	8	0
78.4	28	28	9	10	8	0
78.5	28	28	9	10	8	0
78.6	28	28	9	10	8	0
78.7	28	28	9	10	8	0
78.8	28	28	9	10	8	0
78.9	28	28	9	10	8	0
79	28	28	9	10	8	0
79.1	28	28	9	10	8	0
79.2	28	28	9	10	8	0
79.3	28	28	9	10	8	0
79.4	28	28	9	10	8	0
79.5	28	28	9	10	8	0
79.6	28	28	9	10	8	0
79.7	28	28	9	10	8	0
79.8	28	28	9	10	8	0
79.9	28	28	9	10	8	0
80	28	28	9	10	8	0
80.1	28	28	9	10	8	0
80.2	28	28	9	10	8	0
80.3	28	28	9	10	8	0
80.4	28	28	9	10	8	0
80.5	28	28	9	10	8	0
80.6	28	28	9	10	8	0
80.7	28	28	9	10	8	0
80.8	28	28	9	10	8	0

80.9	28	28	9	10	8	0
81	28	28	9	10	8	0
81.1	28	28	9	10	8	0
81.2	28	28	9	10	8	0
81.3	28	28	9	10	8	0
81.4	28	28	9	10	8	0
81.5	28	28	9	10	8	0
81.6	28	28	9	10	8	0
81.7	28	28	9	10	8	0
81.8	28	28	9	10	8	0
81.9	28	28	9	10	8	0
82	28	28	9	10	8	0
82.1	28	28	9	10	8	0
82.2	27	29	9	11	9	0
82.3	27	29	9	11	9	0
82.4	27	29	9	11	9	0
82.5	27	29	9	11	9	0
82.6	27	29	9	11	9	0
82.7	27	29	9	11	9	0
82.8	27	29	9	11	9	0
82.9	27	29	9	11	9	0
83	27	29	9	11	9	0
83.1	27	29	9	11	9	0
83.2	27	29	9	11	9	0
83.3	27	29	9	11	9	0
83.4	27	29	9	11	9	0
83.5	27	29	9	11	9	0
83.6	27	29	9	11	9	0
83.7	27	29	9	11	9	0
83.8	27	29	9	11	9	0
83.9	27	29	9	11	9	0
84	27	29	9	11	9	0
84.1	27	29	9	11	9	0
84.2	27	29	9	11	9	0
84.3	27	29	9	11	9	0
84.4	27	29	9	11	9	0
84.5	27	29	9	11	9	0
84.6	27	29	9	11	9	0
84.7	27	29	9	11	9	0
84.8	27	29	9	11	9	0
84.9	27	29	9	11	9	0
85	27	29	9	11	9	0
85.1	27	29	9	11	9	0

85.2	27	29	9	11	9	0
85.3	27	29	9	11	9	0
85.4	27	29	9	11	9	0
85.5	27	29	9	11	9	0
85.6	27	29	9	11	9	0
85.7	27	29	9	11	9	0
85.8	27	29	9	11	9	0
85.9	27	29	9	11	9	0
86	27	29	9	11	9	0
86.1	27	29	9	11	9	0
86.2	27	29	9	11	9	0
86.3	27	29	9	11	9	0
86.4	27	29	9	11	9	0
86.5	27	29	9	11	9	0
86.6	27	29	9	11	9	0
86.7	27	29	9	11	9	0
86.8	27	29	9	11	9	0
86.9	27	29	9	11	9	0
87	27	29	9	11	9	0
87.1	27	29	9	11	9	0
87.2	27	29	9	11	9	0
87.3	27	29	9	11	9	0
87.4	27	29	9	11	9	0
87.5	27	29	9	11	9	0
87.6	27	29	9	11	9	0
87.7	27	29	9	11	9	0
87.8	27	29	9	11	9	0
87.9	27	29	9	11	9	0
88	27	29	9	11	9	0
88.1	27	29	9	11	9	0
88.2	27	29	9	11	9	0
88.3	27	29	9	11	9	0
88.4	27	29	9	11	9	0
88.5	27	29	9	11	9	0
88.6	27	29	9	11	9	0
88.7	27	29	9	11	9	0
88.8	27	29	9	11	9	0
88.9	27	29	9	11	9	0
89	27	29	9	11	9	0
89.1	27	29	9	11	9	0
89.2	27	29	9	11	9	0
89.3	27	29	9	11	9	0
89.4	27	29	9	11	9	0

89.5	27	29	9	11	9	0
89.6	27	29	9	11	9	0
89.7	27	29	9	11	9	0
89.8	27	29	9	11	9	0
89.9	27	29	9	11	9	0
90	27	29	9	11	9	0
90.1	27	29	9	11	9	0
90.2	27	29	9	11	9	0
90.3	27	29	9	11	9	0
90.4	27	29	9	11	9	0
90.5	27	29	9	11	9	0
90.6	27	29	9	11	9	0
90.7	27	29	9	11	9	0
90.8	27	29	9	11	9	0
90.9	27	29	9	11	9	0
91	27	29	9	11	9	0
91.1	27	29	9	11	9	0
91.2	27	29	9	11	9	0
91.3	27	29	9	11	9	0
91.4	27	29	9	11	9	0
91.5	27	29	9	11	9	0
91.6	27	29	9	11	9	0
91.7	27	29	9	11	9	0
91.8	27	29	9	11	9	0
91.9	27	29	9	11	9	0
92	27	29	9	11	9	0
92.1	27	29	9	11	9	0
92.2	27	29	9	11	9	0
92.3	27	29	9	11	9	0
92.4	27	29	9	11	9	0
92.5	27	29	9	11	9	0
92.6	27	29	9	11	9	0
92.7	27	29	9	11	9	0
92.8	27	29	9	11	9	0
92.9	27	29	9	11	9	0
93	27	29	9	11	9	0
93.1	27	29	9	11	9	0
93.2	27	29	9	11	9	0
93.3	27	29	9	11	9	0
93.4	26	29	10	11	9	0
93.5	26	29	10	11	9	0
93.6	26	29	10	11	9	0
93.7	26	31	10	11	9	0

93.8	26	31	10	11	9	0
93.9	26	31	10	11	9	0
94	26	31	10	11	9	0
94.1	26	31	10	11	9	0
94.2	26	31	10	11	9	0
94.3	26	31	10	11	9	0
94.4	26	31	10	11	9	0
94.5	26	31	10	11	9	0
94.6	26	31	10	11	9	0
94.7	26	31	10	11	9	0
94.8	26	31	10	11	9	0
94.9	26	31	10	11	9	0
95	26	31	10	11	9	0
95.1	26	31	10	11	9	0
95.2	26	31	10	11	9	0
95.3	26	31	10	11	9	0
95.4	26	31	10	11	9	0
95.5	26	31	10	11	9	0
95.6	26	31	10	11	9	0
95.7	26	31	10	11	9	0
95.8	26	31	10	11	9	0
95.9	26	31	10	11	9	0
96	26	31	10	11	9	0
96.1	26	31	10	11	9	0
96.2	26	31	10	11	9	0
96.3	26	31	10	11	9	0
96.4	26	31	10	11	9	0
96.5	26	31	10	11	9	0
96.6	26	31	10	11	9	0
96.7	26	31	10	11	9	0
96.8	26	31	10	11	9	0
96.9	26	31	10	11	9	0
97	26	31	10	11	9	0
97.1	26	31	10	11	9	0
97.2	26	31	10	11	9	0
97.3	26	31	10	11	9	0
97.4	26	31	10	11	9	0
97.5	26	31	10	11	9	0
97.6	26	31	10	11	9	0
97.7	26	31	10	11	9	0
97.8	26	31	10	11	9	0
97.9	26	31	10	11	9	0
98	26	31	10	11	9	0

98.1	26	31	10	11	9	0
98.2	26	31	10	11	9	0
98.3	26	31	10	11	9	0
98.4	26	31	10	11	9	0
98.5	26	31	10	11	9	0
98.6	26	31	10	11	9	0
98.7	26	31	10	11	9	0
98.8	26	31	10	11	9	0
98.9	26	31	10	11	9	0
99	26	31	10	11	9	0
99.1	26	31	10	11	9	0
99.2	26	31	10	11	9	0
99.3	26	31	10	11	9	0
99.4	26	31	10	11	9	0
99.5	26	31	10	11	9	0
99.6	26	31	10	11	9	0
99.7	26	31	10	11	9	0
99.8	26	31	10	11	9	0
99.9	26	31	10	11	9	0
100	26	31	10	11	9	0
100.1	26	31	10	11	9	0
100.2	26	31	10	11	9	0
100.3	26	31	10	11	9	0
100.4	26	31	10	11	9	0
100.5	26	31	10	11	9	0
100.6	26	31	10	11	9	0
100.7	26	31	10	11	9	0
100.8	26	31	10	11	9	0
100.9	26	31	10	11	9	0
101	26	31	10	11	9	0
101.1	26	31	10	11	9	0
101.2	26	31	10	11	9	0
101.3	26	31	10	11	9	0
101.4	26	31	10	11	9	0
101.5	26	31	10	11	9	0
101.6	26	31	10	11	9	0
101.7	26	31	10	11	9	0
101.8	26	31	10	11	9	0
101.9	26	31	10	11	9	0
102	26	31	10	11	9	0
102.1	26	31	10	11	9	0
102.2	26	31	10	11	9	0
102.3	26	31	10	11	9	0

102.4	26	31	10	11	9	0
102.5	26	31	10	11	9	0
102.6	26	31	10	11	9	0
102.7	26	31	10	11	9	0
102.8	26	31	10	11	9	0
102.9	26	31	10	11	9	0
103	26	31	10	11	9	0
103.1	26	31	10	11	9	0
103.2	26	31	10	11	9	0
103.3	26	31	10	11	9	0
103.4	26	31	10	11	9	0
103.5	26	31	10	11	9	0
103.6	26	31	10	11	9	0
103.7	26	31	10	11	9	0
103.8	26	31	10	11	9	0
103.9	26	31	10	11	9	0
104	26	31	10	11	9	0
104.1	26	31	10	11	9	0
104.2	26	31	10	11	9	0
104.3	26	31	10	11	9	0
104.4	26	31	10	11	9	0
104.5	26	31	10	11	9	0
104.6	26	31	10	11	9	0
104.7	26	31	10	11	9	0
104.8	26	31	10	11	9	0
104.9	26	31	10	11	9	0
105	26	31	10	11	9	0
105.1	26	31	10	11	9	0
105.2	26	31	10	11	9	0
105.3	26	31	10	11	9	0
105.4	26	31	10	11	9	0
105.5	26	31	10	11	9	0
105.6	26	31	10	11	9	0
105.7	26	31	10	11	9	0
105.8	26	31	10	11	9	0
105.9	26	31	10	11	9	0
106	26	31	10	11	9	1
106.1	26	31	10	11	9	1
106.2	26	31	10	11	9	1
106.3	26	31	10	11	9	1
106.4	26	31	10	11	9	1
106.5	26	31	10	11	9	1
106.6	26	31	10	11	9	1

106.7	26	31	10	11	9	1
106.8	26	31	10	11	9	1
106.9	26	31	10	11	9	1
107	26	31	10	11	9	1
107.1	26	31	10	11	9	1
107.2	26	31	10	11	9	1
107.3	25	33	11	11	9	1
107.4	25	33	11	11	9	1
107.5	25	33	11	11	9	1
107.6	25	33	11	11	9	1
107.7	25	33	11	11	9	1
107.8	25	33	11	11	9	1
107.9	25	33	11	11	9	1
108	25	33	11	11	9	1
108.1	25	33	11	11	9	1
108.2	25	33	11	11	9	1
108.3	25	33	11	11	9	1
108.4	25	33	11	11	9	1
108.5	25	33	11	11	9	1
108.6	25	33	11	11	9	1
108.7	25	33	11	11	9	1
108.8	25	33	11	11	9	1
108.9	25	33	11	11	9	1
109	25	33	11	11	9	1
109.1	25	33	11	11	9	1
109.2	25	33	11	11	9	1
109.3	25	33	11	11	9	1
109.4	25	33	11	11	9	1
109.5	25	33	11	11	9	1
109.6	25	33	11	11	9	1
109.7	25	33	11	11	9	1
109.8	25	33	11	11	9	1
109.9	25	33	11	11	9	1
110	25	33	11	11	9	1
110.1	25	33	11	11	9	1
110.2	25	33	11	11	9	1
110.3	25	33	11	11	9	1
110.4	25	33	11	11	9	1
110.5	25	33	11	11	9	1
110.6	25	33	11	11	9	1
110.7	25	33	11	11	9	1
110.8	25	33	11	11	9	1
110.9	25	33	11	11	9	1

111	25	33	11	11	9	1
111.1	25	33	11	11	9	1
111.2	25	33	11	11	9	1
111.3	25	33	11	11	9	1
111.4	25	33	11	11	9	1
111.5	25	33	11	11	9	1
111.6	25	33	11	11	9	1
111.7	25	33	11	11	9	1
111.8	25	33	11	11	9	1
111.9	25	33	11	11	9	1
112	25	33	11	11	9	1
112.1	25	33	11	11	9	1
112.2	25	33	11	11	9	1
112.3	25	33	11	11	9	1
112.4	25	33	11	11	9	1
112.5	25	33	11	11	9	1
112.6	25	33	11	11	9	1
112.7	25	33	11	11	9	1
112.8	25	33	11	11	9	1
112.9	25	33	11	11	9	1
113	25	33	11	11	9	1
113.1	25	33	11	11	9	1
113.2	25	33	11	11	9	1
113.3	25	33	11	11	9	1
113.4	25	33	11	11	9	1
113.5	25	33	11	11	9	1
113.6	25	33	11	11	9	1
113.7	25	33	11	11	9	1
113.8	25	33	11	11	9	1
113.9	25	33	11	11	9	1
114	25	33	11	11	9	1
114.1	25	33	11	11	9	1
114.2	25	33	11	11	9	1
114.3	25	33	11	11	9	1
114.4	25	33	11	11	9	1
114.5	25	33	11	11	9	1
114.6	25	33	11	11	9	1
114.7	25	33	11	11	9	1
114.8	25	33	11	11	9	1
114.9	25	33	11	11	9	1
115	25	33	11	11	9	1
115.1	25	33	11	11	9	1
115.2	25	33	11	11	9	1

115.3	25	33	11	11	9	1
115.4	25	33	11	11	9	1
115.5	25	33	11	11	9	1
115.6	25	33	11	11	9	1
115.7	25	33	11	11	9	1
115.8	25	33	11	11	9	1
115.9	25	33	11	11	9	1
116	25	33	11	11	9	1
116.1	25	33	11	11	9	1
116.2	25	33	11	11	9	1
116.3	25	33	11	11	9	1
116.4	25	33	11	11	9	1
116.5	25	33	11	11	9	1
116.6	25	33	11	11	9	1
116.7	25	33	11	11	9	1
116.8	25	33	11	11	9	1
116.9	25	33	11	11	9	1
117	25	33	11	11	9	1
117.1	25	33	11	11	9	1
117.2	25	33	11	11	9	1
117.3	25	33	11	11	9	1
117.4	25	33	11	11	9	1
117.5	25	33	11	11	9	1
117.6	25	33	11	11	9	1
117.7	25	33	11	11	9	1
117.8	25	33	11	11	9	1
117.9	25	33	11	11	9	1
118	25	33	11	11	9	1
118.1	25	33	11	11	9	1
118.2	25	33	11	11	9	1
118.3	25	33	11	11	9	1
118.4	25	33	11	11	9	1
118.5	25	33	11	11	9	1
118.6	25	33	11	11	9	1
118.7	25	33	11	11	9	1
118.8	25	33	11	11	9	1
118.9	25	33	11	11	9	1
119	25	33	11	11	9	1
119.1	25	33	11	11	9	1
119.2	25	33	11	11	9	1
119.3	25	33	11	11	9	1
119.4	25	33	11	11	9	1
119.5	25	33	11	11	9	1

119.6	25	33	11	11	9	1
119.7	25	33	11	11	9	1
119.8	25	33	11	11	9	1
119.9	25	33	11	11	9	1
120	25	33	11	11	9	1
120.1	25	33	11	11	9	1
120.2	25	33	11	11	9	1
120.3	25	33	11	11	9	1
120.4	25	33	11	11	9	1
120.5	25	33	11	11	9	1
120.6	25	33	11	11	9	1
120.7	25	33	11	11	9	1
120.8	25	33	11	11	9	1
120.9	25	33	11	11	9	1
121	25	33	11	11	9	1
121.1	25	33	11	11	9	1
121.2	25	33	11	11	9	1
121.3	25	33	11	11	9	1
121.4	25	33	11	11	9	1
121.5	25	33	11	11	9	1
121.6	25	33	11	11	9	1
121.7	25	33	11	11	9	1
121.8	25	33	11	11	9	1
121.9	25	33	11	11	9	1
122	25	33	11	11	9	1
122.1	25	33	11	11	9	1
122.2	25	33	11	11	9	1
122.3	25	33	11	11	9	1

Appendix 2: Reactive Molecular Dynamics input files

```
#######################RMD Hemicellulose Pyrolysis####################

# Initialization
units                   real
boundary                p p p
dimension               3
atom_style              charge

read_data               pyromindata2.in
#read_restart           pyrormd.restart.21600000

#comm_style             tiled
#balance                1.1 rcb

pair_style              reax/c NULL safezone 2.0 mincap 200
pair_coeff              * * RMDVanDuin.CHO H C O Ar
pair_modify             tail yes

fix                     10 all qeq/reax 1 0.0 10.0 1.0e-6 reax/c

#########################################################################

#Variables for simulation

variable        temp equal 1500.0


#########################################################################
### Stage 3 (NPT Reactive Molecular dynamics)
reset_timestep          0

compute  pea  all  pe/atom
compute  pea1 all reduce sum c_pea
compute  kea  all  ke/atom
compute  kea1 all reduce sum c_kea

#fix    1 all nve/omp
fix     2 inert npt/omp temp ${temp} ${temp} 10 iso 1.000 1.000 350.0
fix     4 all reax/c/bonds 1000 rmdanalyze.bonds


#restart        200000 pyrormd.restart
dump            rmd all xyz 1000 pyro.rmdanalyze.xyz
dump_modify     rmd sort id element H C O Ar
dump            charge all custom 100000 chargedata.file id type q x y z
dump_modify     charge sort id
dump            maps all atom 1000 rmdanalyze.dump
dump_modify     maps scale no image yes
```

```
#write_data             pyro.rmd
thermo                  1000
thermo_style            one step elapsed time pe ke temp press etotal

timestep                0.1
run                     1200000

restart                 0
run                     0
undump                  rmd
undump                  charge
undump                  TE
undump                  maps

unfix                   1
#unfix                  2
unfix                   10
unfix                   4
#unfix                   5

print                   "NVE RMD completed"
```